Geological Survey of Sweden

3D geological modelling of the Riddarhyttan Ore Field (Fe–Cu–Au–Co–Mo–REE)

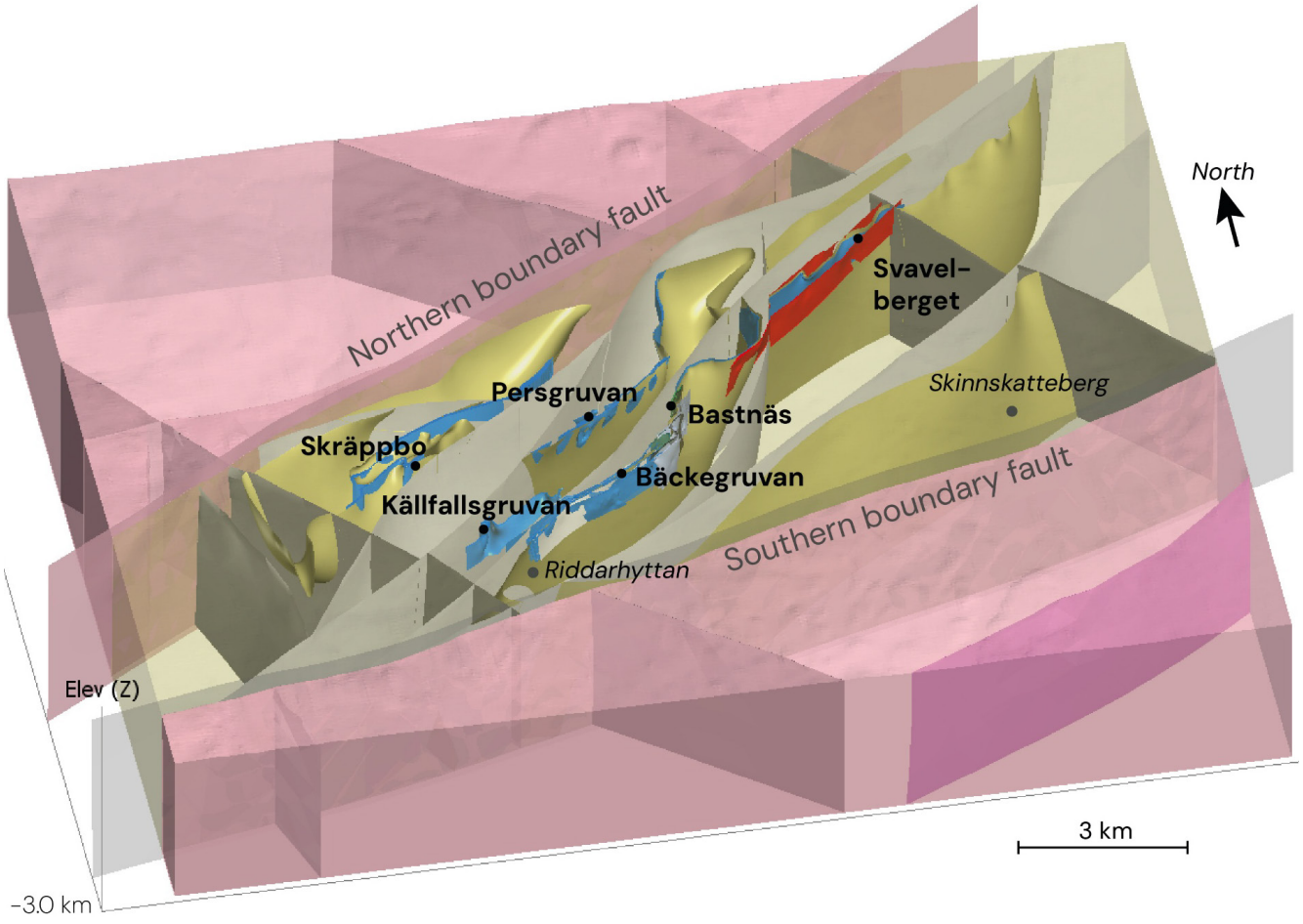

Stefan Luth & Peter Hedin

SGU-rapport 2026:01

www.sgu.se

Author: Stefan Luth & Peter Hedin
Reviewed by: Stefan Bergman
Responsible head of unit: Ann Allen
Editor: Lina Rönnåsen

Cover image: Impression of a 3D-geological model on Riddarhyttan
(Fig. 23 in document).
Illustration: Stefan Luth

Mars 2026

Geological Survey of Sweden
Box 670, 751 28 Uppsala
phone: 018-17 90 00
e-mail: sgu@sgu.se
www.sgu.se

Content

Sammanfattning

Sveriges geologiska undersökning (SGU) har tagit fram en serie geologiska 3D-modeller över berggrunden i Riddarhytte malmfält i Västmanland, vilket inkluderar de historiska gruvorna Bäckegruvan, Östergruvan, Stora Bastnäsgruvan, Källfallsgruvan och Persgruvan. Dessa mineraliseringar innehåller förutom järn, koppar och guld också metaller som kobolt, molybden och REE, vilka betraktas som kritiska av EU.

Modellerna bygger på borrhålsdata och nya strukturmätningar samt geofysisk och geologisk information från SGU:s databaser. En del extern information har erhållits från prospekterings-bolaget EMX Royalty som stöd i tolkning. Totalt har över 336 borrningar bearbetats, med en totalt längd på över 43 kilometer, och lagrats in i modellen. Modellerna visar en tolkad bild av mineraliseringarna, den omgivande berggrunden och strukturer ner till cirka 500 meters djup. En övergripande regional modell går ner till 3,0 kilometer och bygger på djupet enbart på strukturgeologiska koncept.

Modellerna och rapporten syftar till att förstå Riddarhytte malmfälts uppbyggnad och att skapa en översiktlig och sammanhängande bild av de olika mineraliseringarna. Resultatet består av uppdaterad och ny information som kan användas vid mineralprospektering, byggnation eller andra planeringsprojekt i trakten. Modellerna och ingående data finns tillgängliga via www.sgu.se.

Summary

The Geological Survey of Sweden (SGU) has constructed a series of geological 3D models for the Riddarhyttan Ore Field in Västmanland, which includes the former mines Bäckegruvan, Östergruvan, Stora Bastnäsgruvan, Källfallsgruvan and Persgruvan. In addition to iron, copper and gold, these mineralisations also contain metals such as cobalt, molybdenum and REE, which are considered critical by the European Union.

The models are based on drill hole data and new structural measurements as well as geophysical and geological information extracted from the SGU's databases. Additional external information has been obtained from the former exploration company EMX Royalty for the purpose of geological interpretation. In total, over 336 drill holes, with a total length of more than 43 kilometers have been used for this modelling exercise. The resulting models reveal the geometry and size of the individual ore bodies and include the surrounding bedrock and structures down to approximately 500 meters depth. An additional regional model is presented, reaching down to 3.0 kilometers and is based primarily on structural-geological concepts.

The aim of the models and this report is to understand the structure of the Riddarhyttan Ore Field and to create a comprehensive and coherent picture of the different mineralisations at depth. The result comprises updated and new information that is intended to serve mineral exploration, infrastructure or other decision-making projects in the region. The models and input data are available via www.sgu.se.

Introduction

The Geological Survey of Sweden (SGU) has within the scope of the project "Riddarhyttan 3D" constructed geological models for the Riddarhyttan Ore Field in western Bergslagen (Fig. 1). Like the rest of Bergslagen, the mineralisations in the Riddarhyttan area are dominated by iron-oxides but also by copper, gold, cobalt, molybdenum and REE. Most of these metals are ranked "critically" by the European Union (European Commission 2023).

The most recent exploration program that targeted these metals at Riddarhyttan was conducted by former EMX Royalty during 2018–2019 and included extensive field- and drilling campaigns and a high-resolution VTEM survey. With their results obtained, the demand was growing for local- and regional 3D-geological models that can provide insights into the continuation of mineralisations both laterally and at depth. Creating such deposit and regional framework models will also help to better understand the *stratigraphical* build-up, the complex *deformation history*, and interlinked *mineral system*. All this assists in creating new targets for exploration and discoveries in the area.

This report presents local (deposit) and regional 3D geological models for the Riddarhyttan Ore Field. All the models are based on a combination of new and pre-existing geological- and geophysical datasets. Special emphasis is put on new structural data and structural analysis conducted for this study. Deposit-scale models were made for the BIF-magnetite dominated deposits with late Cu-Co-Mo mineralisation including the former Bäckegruvan and Östergruvan mines, the magnetite-skarn deposits including the former Källfallet and Persgruvan mines, and the REE occurrences at the former Bastnäs mines (Fig. 2). An additional model was made of a discordant zone of remobilised massive sulfide, which was more recently drilled by EMX Royalty. A regional model includes all these deposits within a structural framework of major faults and folds. The regional model has a depth range of 3.0 km whereas the deposit models are limited in depth to a few hundred meters.

All modelling was conducted using the software Leapfrog Geo version 2024.1.1. Several of its tools were used to model the high degree of structural complexity present in the Riddarhyttan area. This report can therefore be used as a manual for future projects with an interest in modelling orebodies and structures resulting from polyphase deformation, such as refolded folds and fault networks.

All the models presented in this report are freely available for the public through the SGU's website (www.sgu.se). Also the input data assembled for this study is available through viewers and downloadable databases found through the webservices of the Geological Survey of Sweden.

Geological setting

The Riddarhyttan Ore Field is located in western Bergslagen on the *REE line* (Fig. 1). This is a more than 100 km long and 2 to 6 km wide, northeast-striking belt of metavolcanic rocks with intercalated marble layers and banded iron formation (BIF) (Jonsson & Högdahl 2013, Sadeghi et al. 2019). The volcano-sedimentary sequence is variably sodium, potassium and/or magnesium altered and formed during magmatic activity in a shallow-marine environment within a back-arc basin at c. 1.92–1.88 Ga (Allen et al. 1996). The entire sequence has been polyphase deformed under greenschist to amphibolite facies metamorphic conditions during the Svecokarelian orogeny lasting until 1.8 Ga (e.g. Stephens & Jansson 2020). Deformation was strongly accommodated by the supracrustal rocks and resulted in a zone of high strain, which was referred to by Beunk & Kuipers (2012) as the *West Bergslagen Boundary Zone* (WBBZ), which partly overlaps with the REE line (Fig. 1).

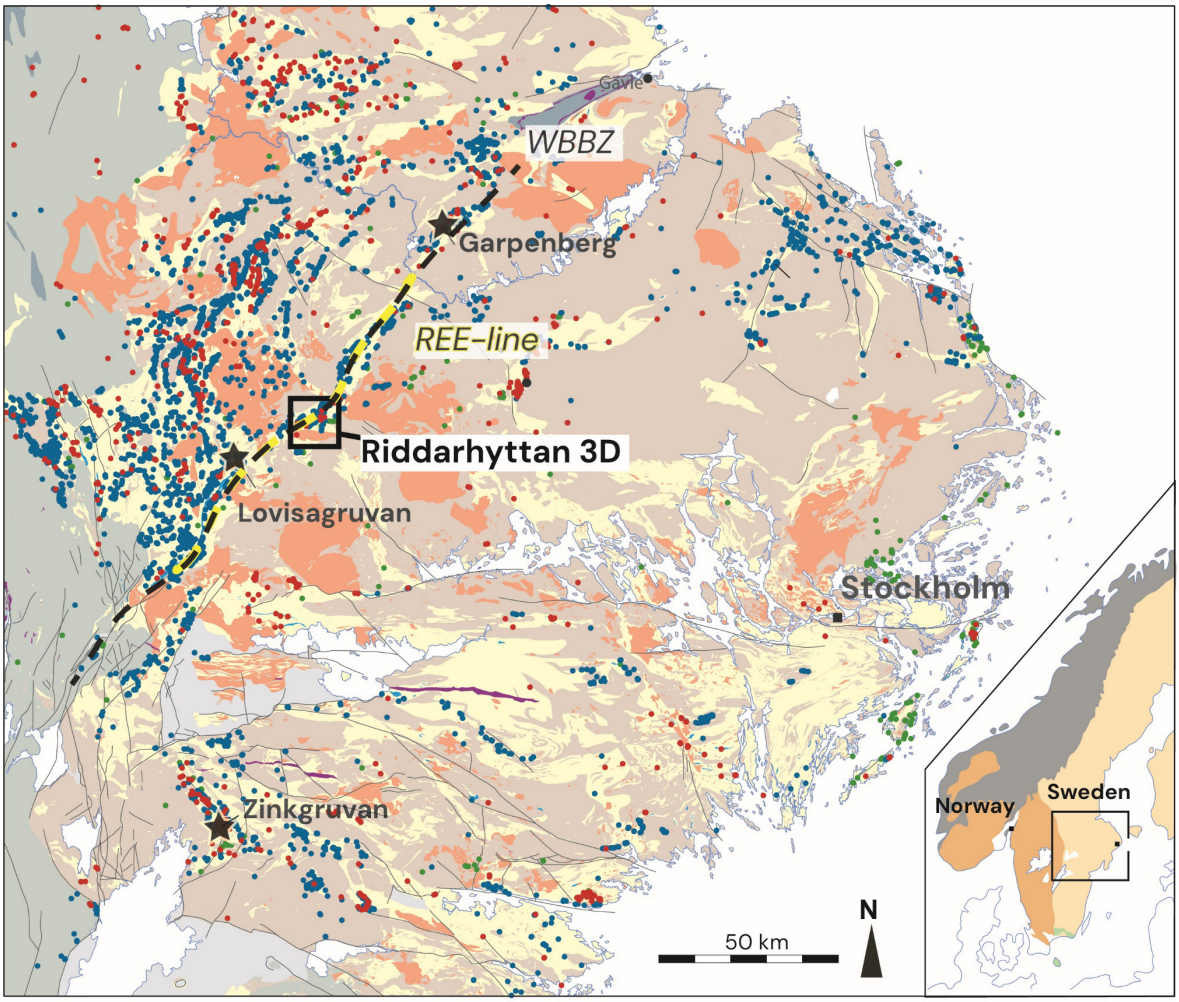

Base metal and other sulphide deposits
Iron oxide deposit
Non-metallic mineral deposits
Active mine (Zn, Pb, Cu, Ag, Au)
Fault, shear zone
Neoproterozoic and Lower Palaeozoic sedimentary rocks
Clastic sedimentary rock (Mesoproterozoic)
Intrusive or meta-intrusive rock suite and associated supracrustal rock (1.81–1.67 Ga)
Intrusive rock suite (1.85–1.75 Ga)
Meta-intrusive rock suites (1.90–1.84 Ga)
Svecofennian metavolcanic and metasedimentary rock
Crystalline carbonate rock

Inset map Scandinavia

Caledonian orogen (0.5–0.4 Ga)
Sveconorwegian orogen (1.1–0.9 Ga)
Svecokarelian / Svecofennian orogen (2.0–1.8 Ga)

Figure 1. Geological map of the Bergslagen ore province showing the location of the Riddarhyttan study area. WBBZ: West Bergslagen Boundary Zone in Beunk & Kuipers (2012). REE line from Jonsson & Högdahl (2013). A detailed map of the study area "Riddarhyttan 3D" is shown in figure 2.

The stratigraphy at Riddarhyttan is largely obscured by a very strong and extensive hydrothermal magnesium alteration, high grade metamorphism, recrystallisation, and intense deformation. Despite the loss of primary structures, early studies have recognised the dominance of laminated rhyolitic ash-siltstones in the area but also the occurrence of quartz-phyric rhyolites and massflow deposits with cm-size pumiceous fragments (e.g. Ambros 1983b; Holtstam et al. 2014; Raat et al. 2020) (Fig. 2).

Intercalated marble layers vary in thickness from a few millimeters to meters and are often affected by magnetite-skarn- or hematite-epidote alteration. With magnetite becoming the dominant mineral, two types of iron-oxide mineralisation are distinguished: magnetite-skarn and laminated banded iron formations (BIF). The former is characterised by massive magnetite with no obvious banding while the BIF is well banded with magnetite layers alternating with mm-thick chert and ash layers. The magnetite-skarn is thought to represent a replacement of former limestone whereas the BIF has more in common with a metamorphosed sedimentary/exhalative style of mineralisation. Both types of magnetite mineralisation are affected by dissemination and cross-cutting stringers of primarily sulfide Cu-Co-Au bearing minerals. A third type of iron-oxide mineralisation is the hematite-BIF, also referred to as "Blåkulla malm", which can be traced for 4–5 km and comprises hematite, chert and calc-sillicate beds.

The REE mineralisations that occur within the Riddarhyttan Ore Field are closely associated with the magnetite-skarns. Moreover, Dunst et al. (2024) has shown that the highest REE concentrations occur along the contact with the metavolcanic rocks as well as along faults. The presence or absence of primary and secondary cesium-bearing minerals further suggests that

1. REE-mineralisation originates from high temperature (≤450 °C) hydrothermal fluids of magmatic origin that reacted with limestone interlayers
2. formation of primary REE silicates predates peak metamorphism and associated ductile deformation
3. faults were used as pathways for REE-rich fluids mainly during late REE remobilisation (Jonsson & Högdahl, 2013; Sahlström et al. 2019; Dunst et al. 2024, Andersson et al. 2024).

Drilling by EMX Royalty in 2019 intersected an ENE-striking zone of massive sulfides consisting primarily of pyrrhotite. The zone, which correlates to the Svavelberget mineralisation at the surface, seems unrelated to a specific host rock or stratigraphic level. Its brecciated textures of angular, cm-sized fragments of foliated and altered wall rock floating within a fine grained pyrrhotite matrix indicates tectonic reworking that post-dates magnesium alteration and main ductile deformation. In addition, Haag et al. (2022) postulates that an alteration assemblage dominated by anthophyllite occurs directly adjacent to the massive sulfide zone and post-dates magnesium alteration and peak metamorphism.

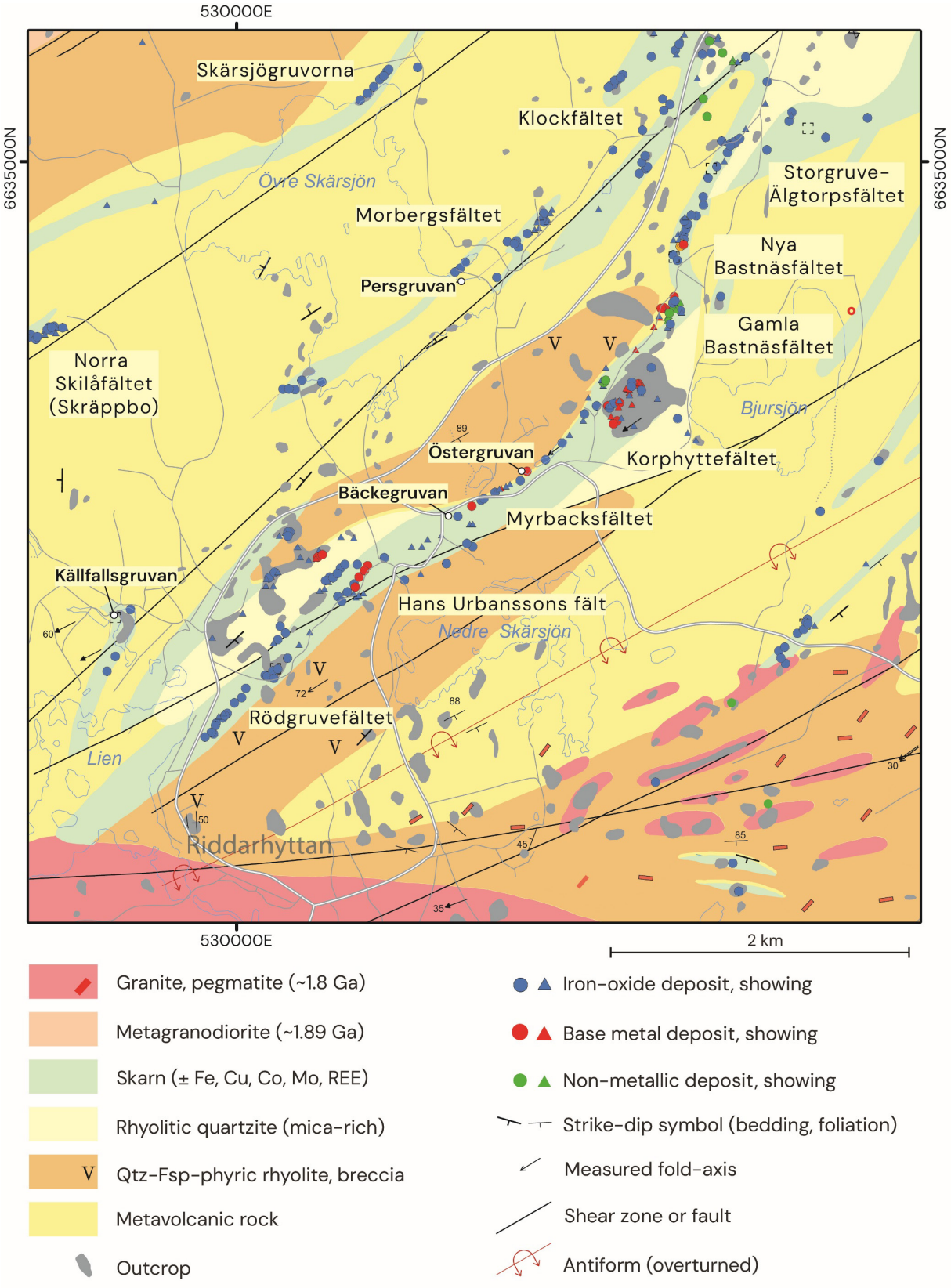

Figure 2. Geological map of the Riddarhyttan Ore Field modified after Ambros (1983a), shown here only as an introduction to the study area. The structural-geological map resulting from our study is shown in figure 24. Coordinates are in SWEREF99TM.

Four samples from the metavolcanic rocks around Bastnäs have been dated by U-Pb geochronology on zircons by Linders (2016) yielding ages between 1899 ± 4 Ma and 1916 ± 4 Ma. The same author suggests ongoing or repetitive magmatism until at least 1820 Ma, based on dated monazite from one of the samples. Age constraints on the timing of mineralisation are limited to Re-Os dating of molybdenite from Bastnäs yielding ages between 1860–1850 Ma (Holtstam et al. 2004). According to Jonsson & Högdahl (2013) these may reflect a large analytical error and are considered too young to be associated with volcanic-magmatic processes.

Structurally, all supracrustal rocks in the Riddarhyttan Ore Field contain a strong penetrative, steeply dipping foliation which strikes predominantly northeast–southwest and parallels stratigraphical contacts. This structural trend mimics the regional trend of the high strain WBBZ. Earlier studies by Geijer & Carlborg (1923), Geijer & Magnusson (1944) and Ambros (1983a) recognised folding of the volcano-sedimentary sequence, but it was Ihre & Sädbom (1986) who interpreted polyphase folding and presented an S-folded Z-fold model for the Korphyttefältet, including Bastnäs. However, at the scale of the entire Riddarhyttan Ore Field the folding pattern is still unresolved due to the lack of way-up indicators and the disruption by shear zones and faults. Kinematic interpretations by Beunk & Kuipers (2012) from several areas in Bergslagen, including Riddarhyttan, related the asymmetric S-folds to sinistral transpression along the WBBZ during D2 deformation. Alternative interpretations on the deformation history based on the results from our study are presented in the chapter *Discussion: Conceptual kinematic model* in this report.

Mining history, exploration and mapping activities

It is unclear exactly when and where mining in the Riddarhyttan area started but the oldest documents related to mining activities under the Crown of Sweden date back to 1420 (Söderhielm et al. 2023). It was Jakob Urbansson who was given the rights in the year 1614 to mine copper at what is today called the "Hans Urbansson field", named after his brother. During the following centuries new fields were discovered, such as Lerklockan and Myrbacksfältet, and ownership changed many times (Fig. 2). Their main interest was copper but shifted towards iron by the end of the 19th century when the company Riddarhytte Aktiebolag was founded and the Källfallet iron deposit was discovered (Geijer & Carlborg 1923). Copper was then only mined as a by-product at Bäckegruvan. The Källfallet mine was continuously active until 1967, whereas the other surrounding mines reopened only periodically during World War I and II. After that the Bäckegruvan mine remained active until 1979.

The total production for the Riddarhyttan Ore Field between 1731 and 1979 is estimated to be around 15 Mt iron ore (50–60% Fe) and 0.12 Mt copper ore (Bergquist, 1985). A resource estimate from Fagersta AB in 1978 gave 13 Mt iron ore (~35% Fe) of which 9.5 Mt at Bäckegruvan and 3.5 Mt at Persgruvan and Lerklockan (Bergquist 1985). See also chapter *Discussion: A future resource?* in this report.

Exploration activities in the Riddarhyttan Ore Field continued directly after mine closure in 1979. As a last resort to extend the life of the mine, two exploration drifts of 2.2 km in total length were built at the -360 m level from Myrbacksfältet to Persgruvan and between Östergruvan and Nya Bastnäs. 6.5 km of horizontal drilling from these drifts did not result in new discoveries and it was decided in 1982 to flood the entire underground mining infrastructure.

After the permanent closure several exploration companies have been active in the Riddarhyttan area. On commission by Swedish government, Sveriges Geologiska AB conducted ground geophysical surveys (magnetics and electro-magnetics), geologyical fieldwork and some drilling

mainly in the Korphyttefältet between 1984 and 1987 (Ihre & Sädbom 1986). Field mapping and sampling of outcrops, boulders and till continued again in the early 2000s by Lake Resources. Four holes were drilled based on a new VTEM survey over Pellegruvan by Boliden in 2006. In the same year International Gold Exploration AB conducted both ground surveys (IP and EM) and drilled seven shallow holes outside the main iron ore trend focusing on Au, Cu and REE. Dannemora Mineral AB was active in the Riddarhyttan area between 2008 and 2014. They re-assayed 67 legacy holes with the intention to construct a 3D resource model of the historic iron mines. Botnia Exploration AB conducted ground geophysics (data not reported to Bergsstaten) and drilled three holes in the northeastern part of the area during the period 2010–2013 with focus on REE.

EMX Royalty conducted a greenfield exploration program between 2018 and 2019. The program included an extensive field campaign, structural mapping and sampling for lithogeochemistry from outcrops. A high-resolution VTEM survey was executed and generated targets for drilling and field observations. A total of 15 relatively deep holes were drilled measuring approximately 5.5 km in length and gave interesting results (Raat 2020).

SGU has published several maps and reports on Riddarhyttan written mostly in Swedish. Relevant in particular for our study are the publications and maps by Tegengren (1912, 1924), Geijer (1921), Geijer & Carlborg (1923) and Geijer & Magnusson (1944). The most recent bedrock map covering the study area at scale 1:50 000 was published by SGU in the early 1980s directly after the mine closures (Ambros 1983a, 1983b)(Fig. 2). More recently, SGU conducted an inventory of all the mineral occurrences within the area and surroundings (Söderhielm et al. 2023). All the SGU reports and maps are downloadable and the associated mineral and drillhole databases can be viewed through the SGU's website (www.sgu.se).

Other useful (mine) maps and reports that have been used for our 3D modelling exercise were extracted from exploration reports (e.g. Bergquist 1985, Ihre & Sädbom 1986) and recent scientific publications (e.g. Sahlström et al. 2019, Dunst et al. 2024). More details on these datasets are provided in the chapter *Model input data*.

Methodology and modelled volumes

The main datasets used for this study were geological and geophysical maps, outcrop observations including structural measurements, drill data and mine level maps (Table 1). The bulk of the structural data used has been collected by SGU in 2020 within the scope of this project. Airborne geophysical acquisition was conducted by SGU in 2016 and 2017 and includes magnetic, electromagnetic and spectrometric data. The remaining datasets were extracted and compiled from SGU databases and exploration reports. All used geophysical datasets are downloadable via the webservices at www.sgu.se.

Modelling was performed using the software Leapfrog Geo version 2024.1.1, which is an implicit 3D geological modelling software that is frequently used in the mining, exploration, groundwater contamination, and geothermal energy industries. The software contains tools that combine constraints from various geological and geophysical datasets within a logical workflow, allowing continuous updates and refinements of the models. Information about Leapfrog and its tools can be found at www.seequent.com.

The deposit-scale models were constructed using primarily the tool named *Vein modelling,* where specific ore intervals were selected from the drill data and subsequently modelled as 3D veins through FastRBF™ interpolation (Fig. 3, Table 1).

This selection of the ore intervals was done manually and directly in 3D, with a focus on the general trend and avoiding details. This implied grouping of logged lithologies and lumping of the different ore types into magnetite ore, hematite BIF, and sulfide ore. Typically, interlayers of volcanic rocks and skarn thinner than 1 meter were included within the ore interval, whereas thicker intervals of similar lithologies and often logged as "containing some disseminated magnetite or sulfides", where excluded and considered as wall rock.

Subsequently, many ore veins modelled from solely drill data were modified by adding additional constraints from other datasets. As such, the correlation between strong positive magnetic anomalies and iron mineralisation has been used to adjust the map trace of the modelled vein. In a similar way, the positive VTEM anomaly was used to constrain the "massive sulfide vein" of the Svavelberget model. At depth, extra map traces, or so-called polylines, were drawn from mine-maps on which lithological contacts were constrained by tunnel mapping in combination with drill data.

Structural data from outcrops and drill cores were used as a final step to refine the geometry of the modelled veins. This was done by first modelling a so-called structural surface, which is based on non-contact structural measurements and may be considered the 3D version of a form-line that shows a structural pattern. Since a structural surface is highly sensitive to data outliers and local disturbances, we created synthetic structural data that represented the average orientation of a cluster of real structural measurements.

Finally, faults have been added to some of the models (Table 1). For the deposit-scale models, faults were mostly interpreted from observable offsets between the various drill markers, while in the regional model, faults were modelled directly from 2D lineaments that were interpreted from magnetic and electromagnetic anomaly maps. Note that the faults in the regional model are unconstrained at depth and that a sub-vertical dip for the first two kilometers is only assumed.

The regional model includes all the modelled deposits and consists of multiple fault blocks that include folding patterns of structural surfaces interpolated from strike-dip measurements obtained from outcrops and drill cores. The depth extents of the regional model is 3.0 kilometers, whereas the deposit models measure typically 500 to 750 meters in depth (Fig. 3, Table 1).

Table 1. Summary of the deposits presented in this report.

3D model	Size	Data	Method/Technique
Korphyttefältet–Bastnäsfältet	L: 1.8 km W: 1.1 km D: 700 m	Drill data, -360 m level map, structural data from outcrops, geological maps from Geijer & Carlborg (1923), Ihre & Sädbom (1986) and EMX, magnetic anomaly map.	**Leapfrog Geo tools:** Vein modelling guided by structural surfaces including synthetic structural data. Offset deposit surfaces. Faulted model.
Persgruvan-Lerklockan	L: 3.0 km W: 2.1 km D: 600 m	Drill data, mine maps, structural data from outcrops and oriented drilling (EMX), magnetic anomaly map, SGU mineral database.	**Leapfrog Geo tools:** Vein modelling including manual adjustment of vein borders. Faulted model.
Bäckegruvan-Östergruvan-Pellegruvan	L: 2.6 km W: 1.9km D: 550 m	Drill data, mine maps, structural data from outcrops and oriented drilling (EMX), magnetic anomaly map.	**Leapfrog Geo tools:** Vein modelling including vein network and adjustment of reference plane by structural data from drilling.
Källfallsgruvan	L: 2.0 km W: 1.2 km D: 500 m	Mine maps (Sundholm, 1899-1971), previous modelled surfaces and structural data from outcrops (Spahic, 2021), magnetic anomaly map.	**SKUA-GOCAD tools:** Surface from closed polygons. **Leapfrog Geo tools:** Vein modelling guided by structural surfaces including synthetic structural data.

Table 1. Continued.

3D model	Size	Data	Method/Technique
Svavelberget	L: 4.5 km W: 4.0 km D: 750 m	Drill data and VTEM (primarily from EMX), SGU mineral database.	**Leapfrog Geo tools:** Vein modelling guided by structural surfaces. Faulted model.
Skrappbo synform	L: 7.5 km W: 5.8 km D: 600 m	Magnetic anomaly map, SGU bedrock map (Ambros, 1983a), SGU mineral database.	**Leapfrog Geo tools:** Vein modelling guided by structural surfaces and synthetic structural data.
Regional 3D fault block model	L: 19 km W: 15 km D: 3 km	Lineaments based on geophysical interpretations.	**Leapfrog Geo tools:** Multi-faulted geological model using fault chronology.
Regional 3D structural model + mineral deposits	L: 19 km W: 15 km D: 3 km	Lineament map, structural data, SGU bedrock map (Ambros, 1983a), way up indicators, SGU mineral database, magnetic anomaly map.	**Leapfrog Geo tools:** Structural Surfaces. Multi-faulted geological model. Import meshes from local models.

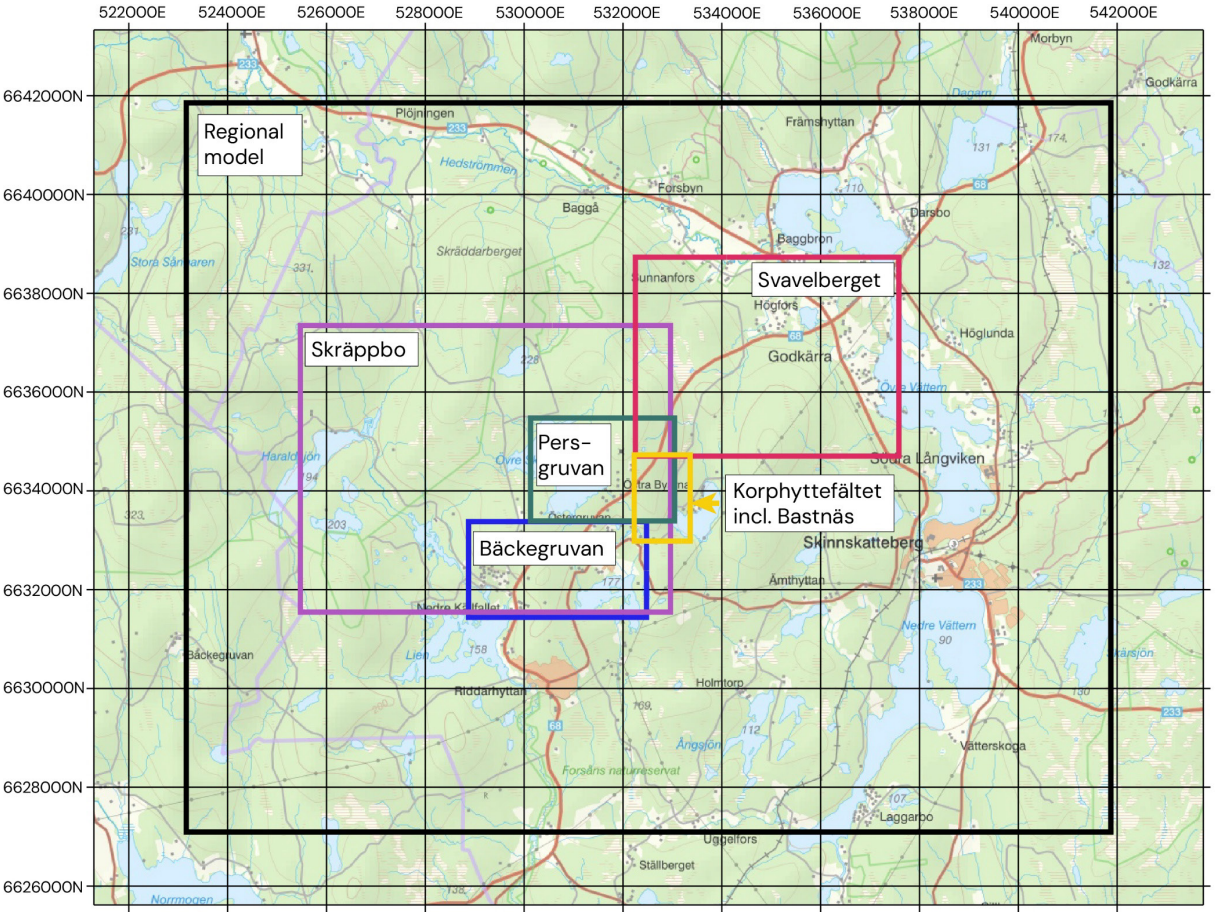

Figure 3. Outline of the individual models presented in this report. Coordinates are in SWEREF99TM and one grid square equals 2 kilometres.

Model input data

Regional geophysics

Regional magnetic, electromagnetic and spectrometric data was acquired by SGU in an airborne survey in the Riddarhyttan area in 2016 and 2017. These surveys were flown at a nominal altitude of 60 m and with a flightline separation of 200 m and azimuth of 130 degrees from the north. Aeromagnetic data was acquired with a 1 nT accuracy and a point separation of c. 7 m along the flight lines. After reducing the total magnetic intensity field (TMI) to the geomagnetic north, an anomaly map was calculated as the difference between the TMI and a 1 km upward continuation of the TMI and is shown in Figure 4. Positive anomalies (red hues) show areas with stronger magnetic properties, which are often linked to ferro- and ferrimagnetic minerals (such as magnetite) in, for example, volcanic-sedimentary rocks or mafic intrusive rocks. In Riddarhyttan, a clear correlation is seen between the iron-rich mineralisations and strongly positive magnetic anomalies.

The electromagnetic field was investigated in the VLF frequency band (Very Low Frequency, 15–30 Hz) where the signal from two transmitters was recorded with a point separation of approximately 15 m along the flight lines. This gives information on subsurface resistivity that can be used to calculate directionally independent maps of apparent electrical resistivity (Fig. 5) and current density. Blue hues indicate low electrical resistivity (high electrical conductivity) which may indicate the presence of, for example, electrically conductive mineralisations or water-bearing formations or structures. However, it can also be the response from for example lakes, rivers, creeks and infrastructure. The majority of the mineralisations in the Riddarhyttan area lie in zones of low apparent electrical resistivity, however, it should also be noted that power lines are located along some of the mineralised horizons where mining operations have been active in the past, which affects interpretation and modelling of the electromagnetic data locally.

A total of 391 new gravity measurements were made by SGU in the project area in 2020. Combined with the previously available gravity data in the SGU databases, this increased the measurement point density from c. 1/km^2 to c. 2/km^2 regionally, and up to 10/km^2 locally in the vicinity of the Riddarhyttan mineralisations. A gravity anomaly map, calculated as the difference between the Bouguer anomaly and a 3 km upward continuation of the Bouguer anomaly, is shown in Figure 6. In general, mafic rocks as well as some mineralisations, have relatively high density and give rise to positive gravity anomalies that indicate local mass excesses (red hues). Felsic rocks generally have relatively low densities and give rise to negative gravity anomalies or local mass deficits (blue hues). The Riddarhyttan area is dominated by a mass excess clearly linked with the iron-rich mineralisations.

A total of 68 petrophysical samples were collected within the project. These are plotted in Figure 7 together with 138 previously measured samples from the area. 86 previously measured samples that are missing information about the rock type have been excluded from this study.

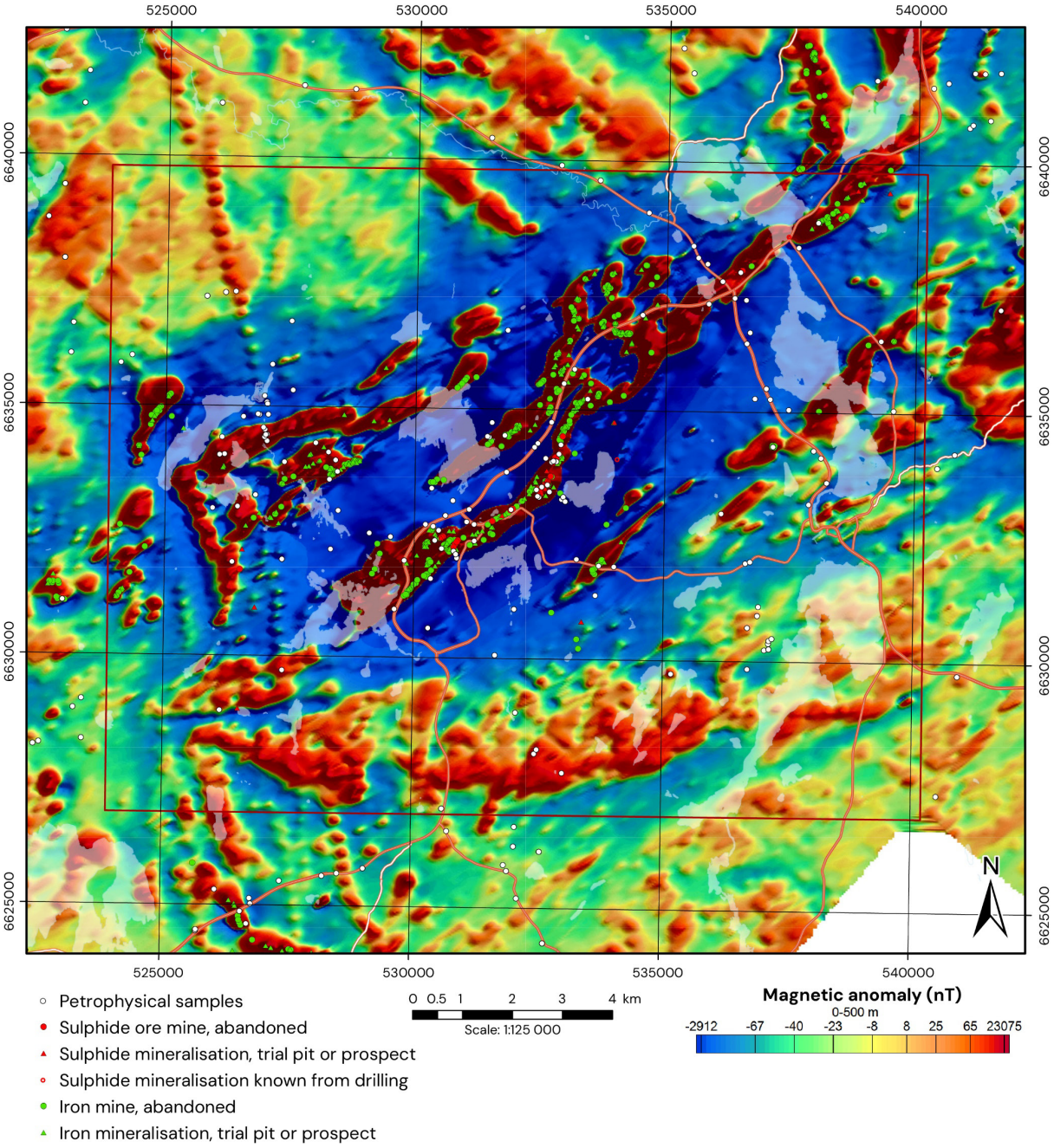

Figure 4. Magnetic anomaly map based on airborne data acquired in 2016–2017 reduced to the geomagnetic north. The map was calculated as the difference between the total magnetic field and a 1 km upward continuation of the total magnetic field. Semitransparent white areas are lakes.

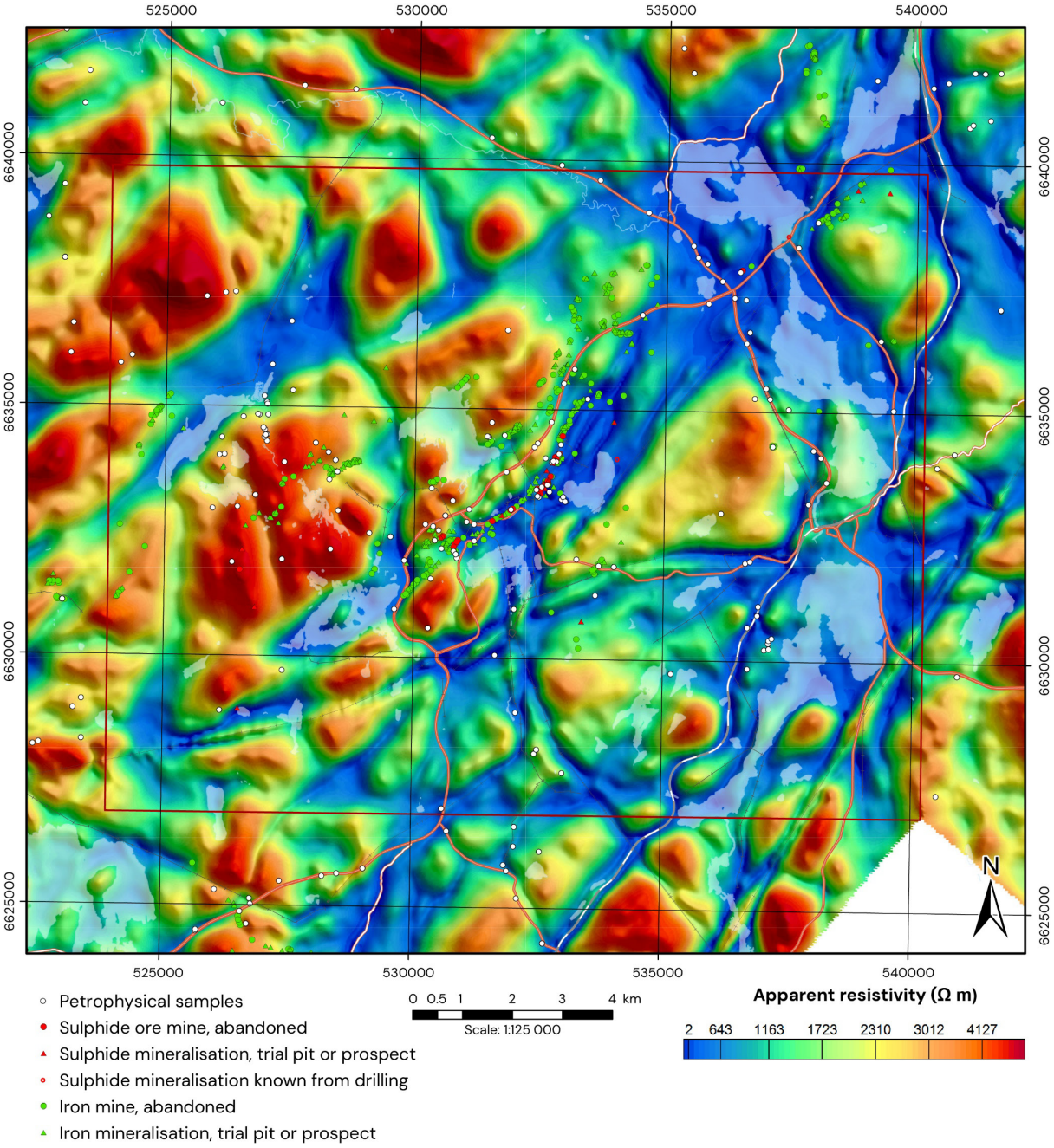

Figure 5. Apparent resistivity map based on airborne data acquired in 2016–2017. Semitransparent white areas are lakes.

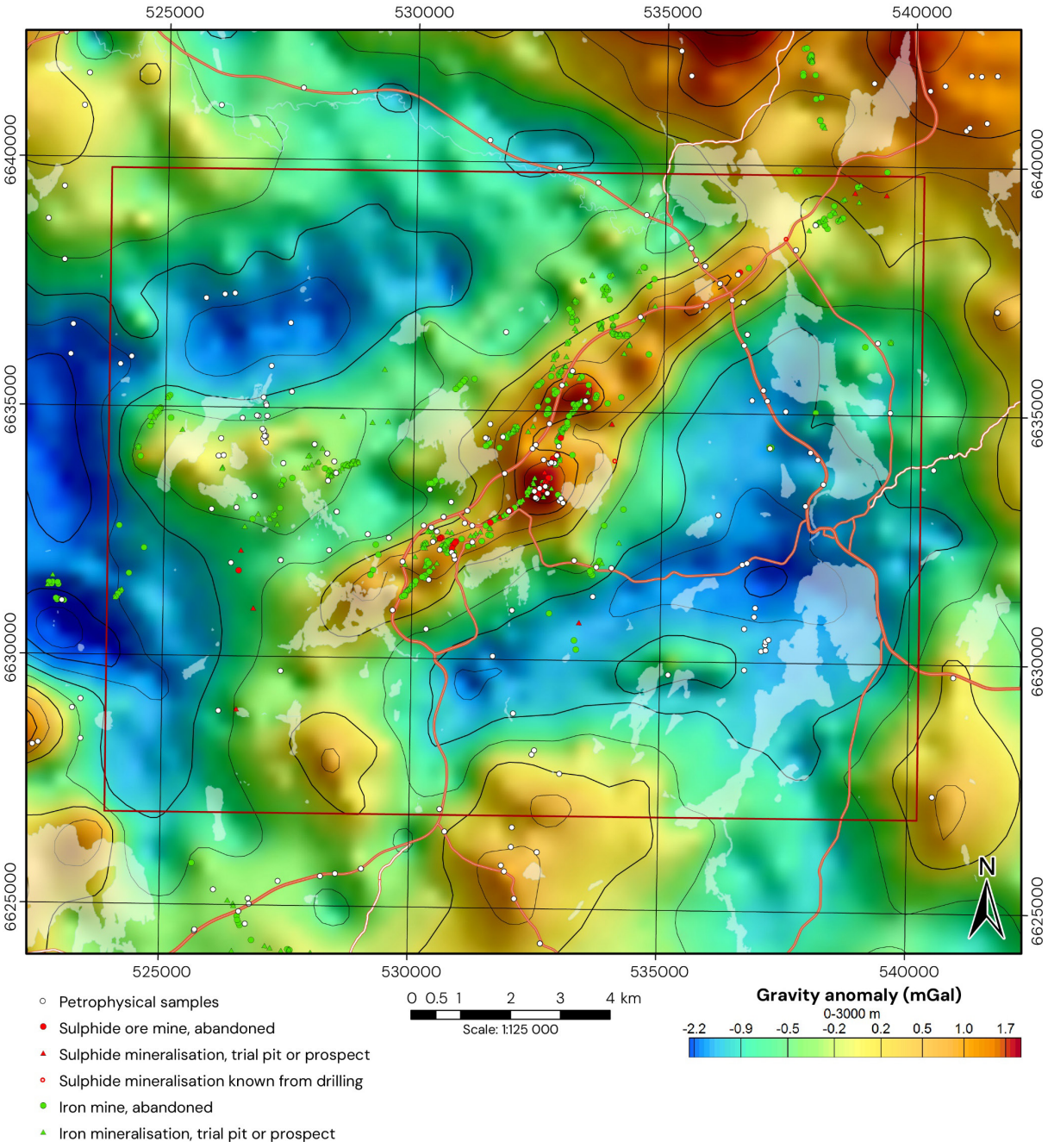

Figure 6. Gravity anomaly map based on all available data, including new data acquired for the project in 2020. The map was calculated as the difference between the Bouguer anomaly and a 3 km upward continuation of the Bouguer anomaly. Semitransparent white areas are lakes.

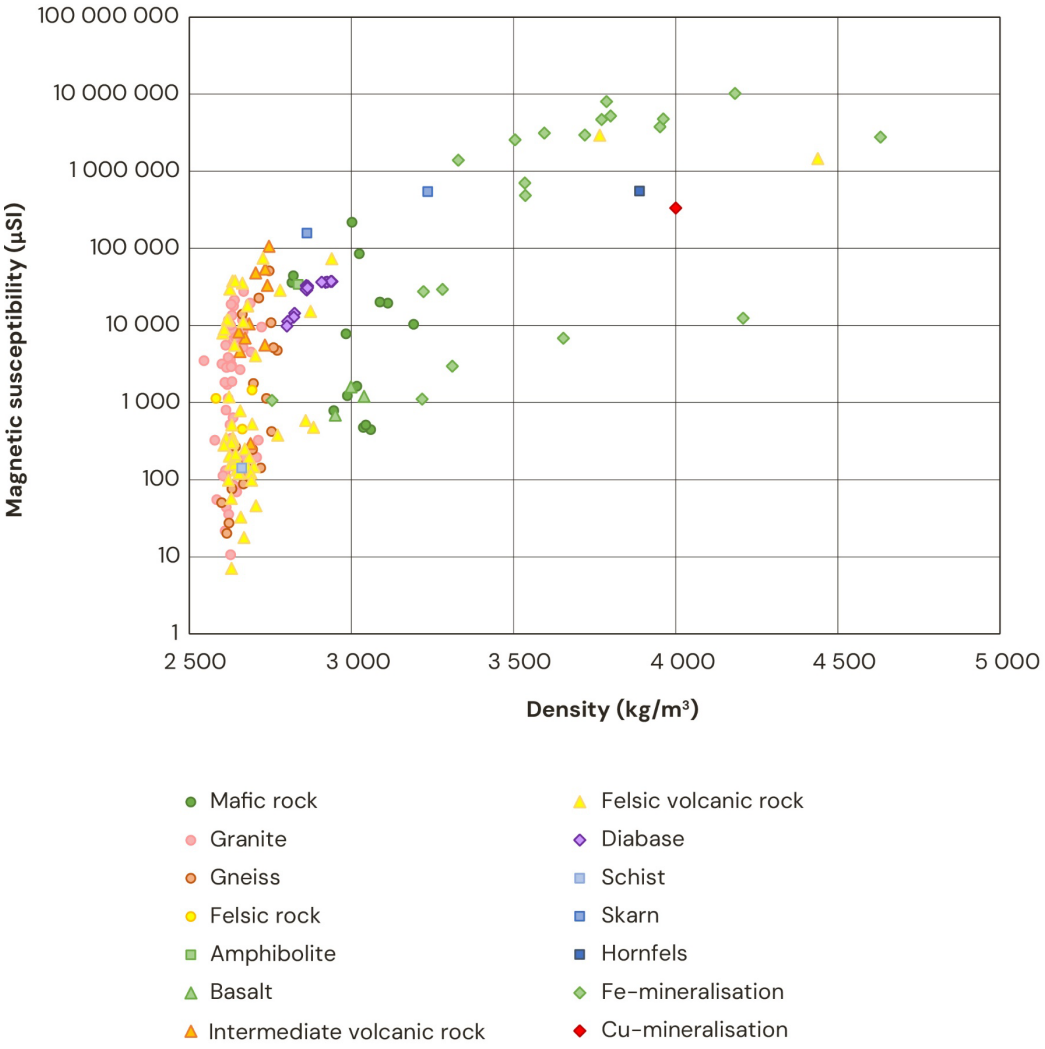

Figure 7. The distribution of magnetic susceptibility versus density among the 206 samples from within the Riddarhyttan area of interest.

New fault map from lineaments

Lineaments were interpreted manually from both the magnetic anomaly map and apparent resistivity map (Figs. 4 and 5). Some of the lineaments have been interpreted after applying filters to the anomaly maps, while others were derived from the apparent offset of high anomaly zones. Note that many low resistivity zones are associated with anthropogenic infrastructure (e.g. power lines and railroads, see Fig. 5) and these are not considered as lineaments in a geological context.

Most lineaments are interpreted as faults, which typically correlate with zones of magnetic lows and/or low resistivity, varying in length between one to tens of kilometers (Fig. 8). The resulting fault map reveals a contrasting structural pattern between the sedimentary-volcanic rock domain and the intrusive rock domain (Fig. 8). NNE to NE-striking faults prevail in the former and are largely absent in the latter, whereas NW-striking faults are present in both domains. This overall structural pattern appears even on the gravity anomaly map (Fig. 6), with a sigmoid-shaped gravity high in the sedimentary-volcanic rock domain. The continuation of and the intersection between different faults appears straightforward in most places, with in general NNE to NE-striking faults cutting-off or even displacing the NW-striking faults. This does not automatically constrain the relative age of the structure more than that the former has likely been active longer compared to the latter.

Following the modelling procedure, all the faults shown in Figure 8 have been inserted as "fault traces" within the 3D fault block model and the regional model (see chapter *Modelling results*).

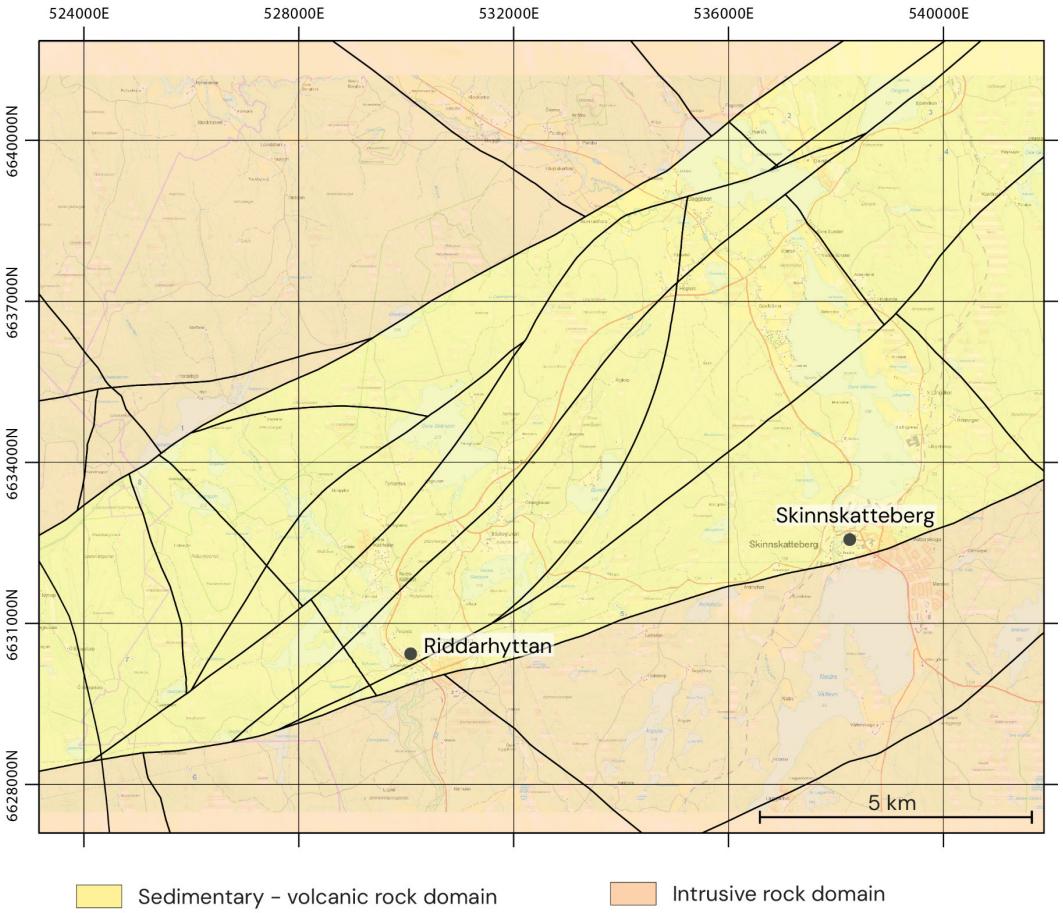

Figure 8. Fault map interpreted from the magnetic anomaly- and apparent resistivity maps (Figs. 4 and 5). The main NE-striking high strain belt is dominated by sedimentary and volcanic rocks. Brownish color refers to the domain outside the high strain belt comprised mainly of granitic rocks.

Outcrop observations and structural data

The main structures observed in outcrops as well as in thin-sections from the Riddarhyttan Ore Field are planar S_0 and S_1 foliations that are mostly parallel, stretching lineations ($L_{stretch}$), asymmetric folds, C-S shear fabrics, boudinage and fractures (Figs. 9 and 10).

Bedding (S_0) varies from massive to medium thick beds (Fig. 9A) to very thin alternating laminae (Figs. 9F–G). However, in many of the rhyolitic volcanic rocks as well as the massive magnetite ores and skarns, bedding planes did not develop or are obscured by a tight metamorphic banding which we labeled as S_1 or S_0/S_1 if indistinguishable. Within the mica-rich volcanic rocks that envelope the ore deposits both to the north and to the south, S_1 developed as a schistose- to mylonitic foliation that often contains a well-developed stretching lineation, which varies in scale from mineral grains to dm-sized clasts or boudins (Fig. 9B). C-S fabrics, indicating shearing, were also observed in outcrops of similar rock type (Fig. 9D). Microstructures include mica-fish, C-S fabrics, strong crenulation fabrics, and rotated clasts, all revealing intense shearing (Fig. 10).

Asymmetric folds occur both as Z- and S-folds – even within the same outcrop – with amplitudes and wavelengths ranging from a few centimeters to a few hundred meters (Fig. 9E–F and 10E–F). Mesoscopic folding is most intense in the hematite BIF (Blåkullamalm), wherein many of the smaller folds are interfolial in character (Fig. 9F). Individual skarn beds that occur in the volcanic sequence are also typically folded asymmetrically, indicating non-coaxial shearing. Some key localities have revealed polyphase folding where a Z-fold is refolded by an S-fold (Fig. 9G). Such folding mimics the much larger folding pattern of the Korphyttan area as mapped by Ihre & Sädbom (1986).

Throughout the Riddarhyttan Ore Field, S_0 and S_1 foliations are striking mostly NE-SW and are typically steeply dipping (Fig. 11). Stretching lineations are predominantly trending towards the southwest with a plunge between 35 and 80 degrees. The bulk of the folds in outcrop have subvertical NE-striking axial planes with fold axes plunging moderately steep to the southwest (Fig. 11).

The types, number and origin of structural measurements from outcrops that have been used in this study for 3D geological modelling are listed in Table 2. All measurements were collected in 2019 and 2020, by SGU, two students from Luleå Technical University (LTU), and by EMX Royalty.

Table 2. Type and number of structural measurements from outcrop used for this study.

Structure-type	SGU	LTU student (Spahic)	LTU student (unpublished)	EMX Royalty
Foliations	198	68	106	92
Stretching lineations	63	5	13	32
Fold axis	19	0	0	18

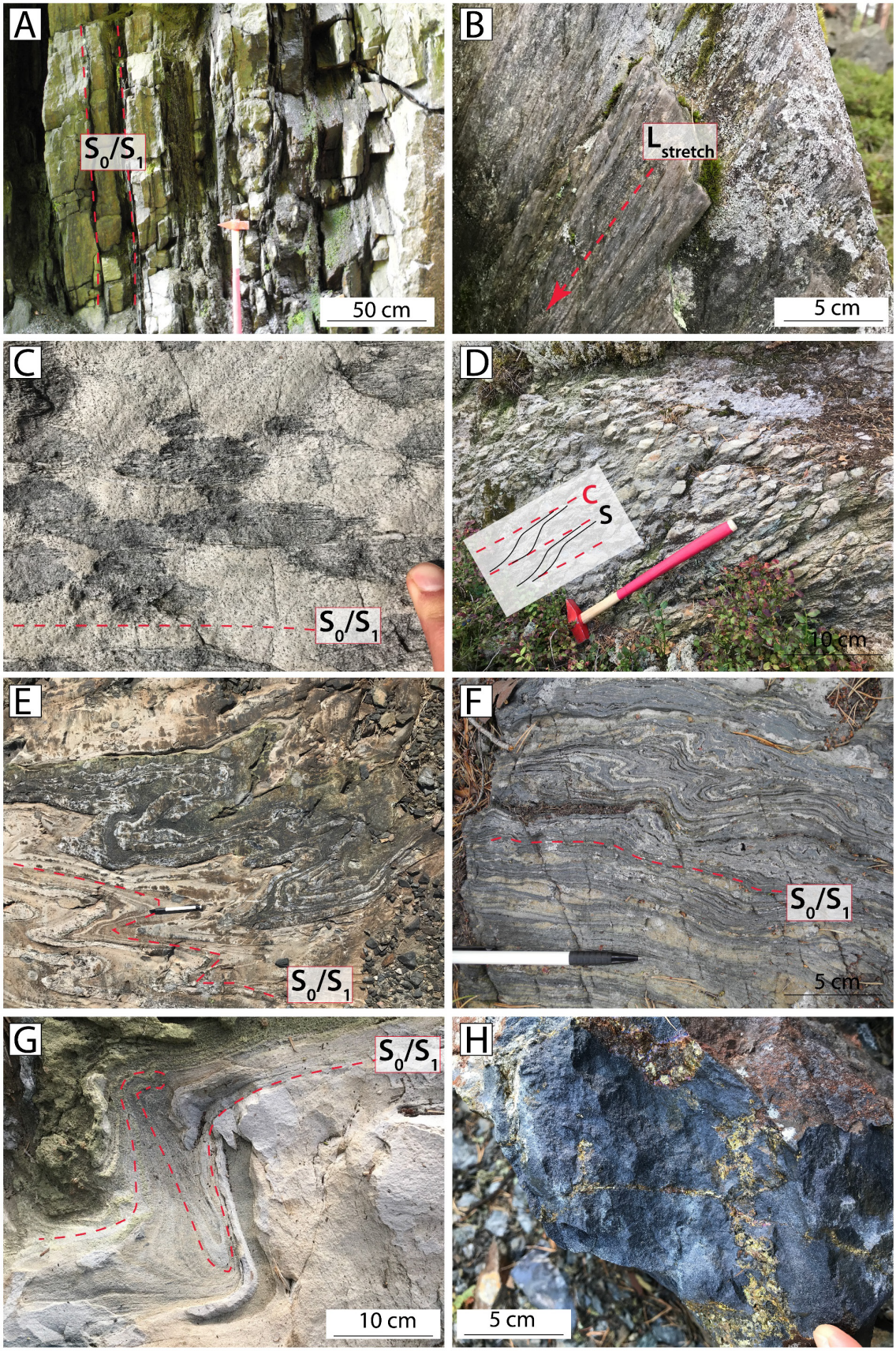

Figure 9. A–G. Structures in outcrops from the Riddarhyttan Ore Field. See the main text for more information. **H.** Orthogonal Cu-Co-sulfide veins within magnetite ore from Bäckegruvan.

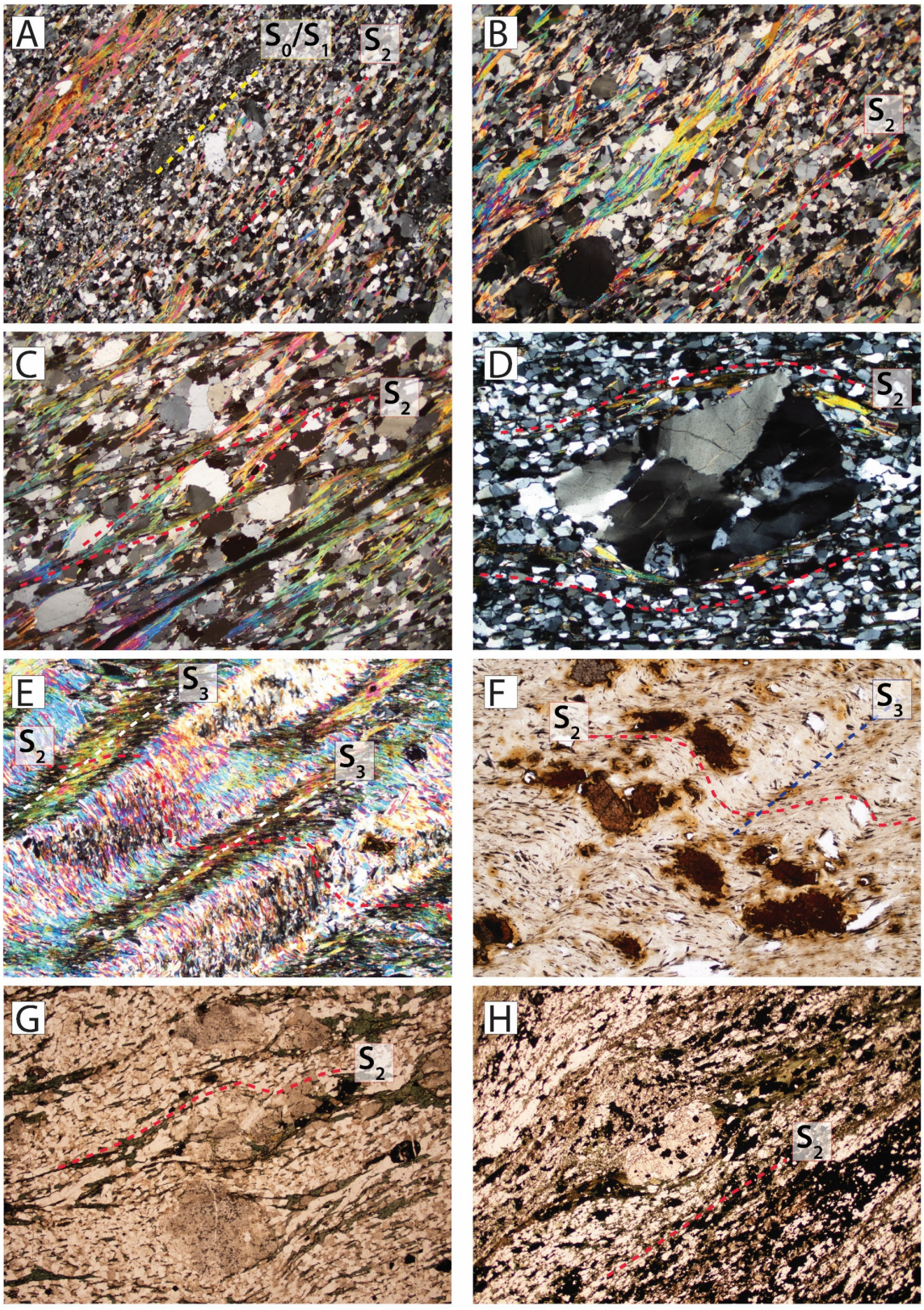

Figure 10. Character of microstructures in metavolcanic rocks from the Riddarhyttan Ore Field. **A–C.** Compositional banding interpreted as S_0/S_1 of mainly recrystallised quartz alternating with minor biotite and muscovite. S_2 is defined by the local alignment of biotite and muscovite. **D.** Rotated clast revealing dextral shearing (top-to-the-right). **E–F.** Micaceous schist showing crenulation cleavage (S_3) and asymmetric folding consistent with dextral shearing (top-to-the-right). **G–H.** Sheared, magnesium-altered schist including chlorite (green) and magnetite (opaque) defining S_2 warping around cordierite pseudomorph blasts. The width of each photo scales 6 millimeters. Cross-polarized light in A–E. Plane-polarized light in F–H.

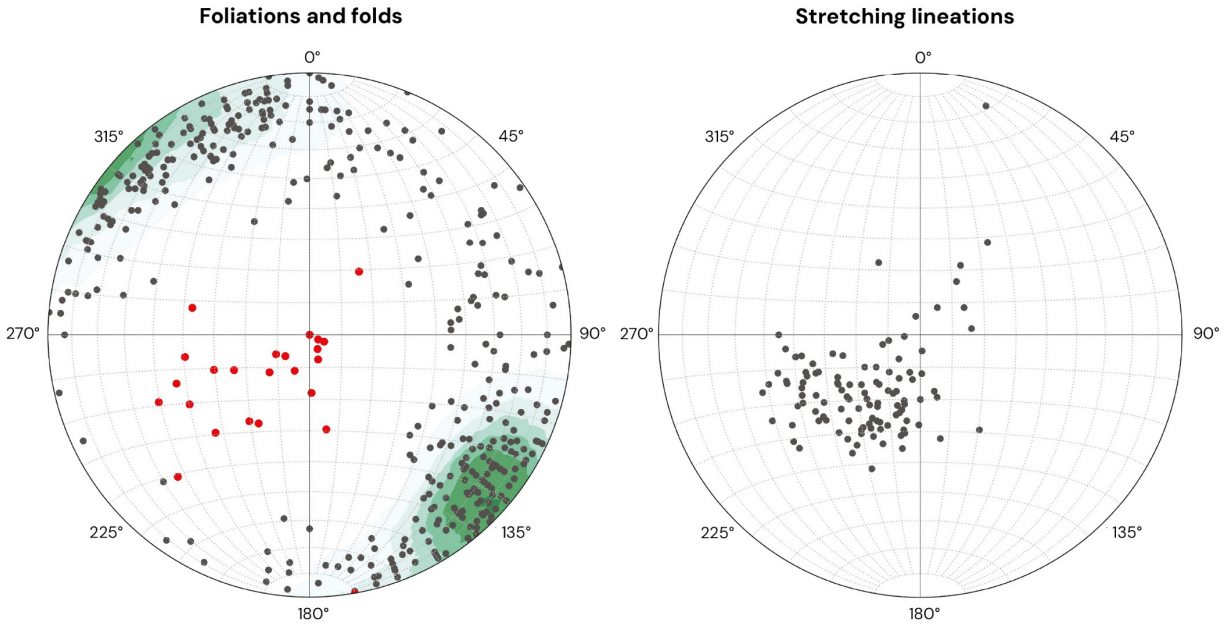

Figure 11. Structural measurements from outcrops projected in lower-hemisphere, equal area stereonets. Foliations plotted as poles (n: 469) include compositional banding. Contouring of data is at a 5σ significance level using Kamb from the method Kamb (1959). Fold-axes (n: 37) are plotted in red. Stretching lineations (n: 113) are plotted in the diagram to the right.

Drill data

In total, data from 336 drillholes from the Riddarhyttan Ore Field was used for 3D geological modelling (Table 3, Figs. 12 and 13). The bulk was drilled underground during and after mining operations throughout the 1960s to 1980s shortly before the tunnels were finally flooded. The drillholes from the ground surface are typically longer, with a median length of 207 meters, reaching maximum drill depths of 670 meters in the EMX Royalty drilling campaigns during 2019. Those are exploration holes that are well-distributed throughout the study area, whereas the bulk of the legacy drill holes, which were drilled by various companies, are restricted to the historic mines such as Bäckegruvan and Östergruvan. An additional large number was drilled from the exploration tunnels at the -360 m level at Korphytte-Bastnäs and to a lesser extend from the tunnel between Östergruvan and Persgruvan (Fig. 13). More information on the drill data, such as previous owner, exact year of drilling, location of core storage at present, and the coinciding protocol and log descriptions can be found on www.sgu.se.

Data was extracted from the original drill logs and digitised into spreadsheets by SGU, EMX Royalty and the voluntary worker Bengt Högrelius. A relatively small amount of drillhole logs lacked data on drill locality or orientation, and those were therefore excluded from the 3D modelling exercise. No drill core has been sampled or re-logged for this study.

The spreadsheets containing the drill data were imported into Leapfrog Geo as so-called collar, survey and interval files (Fig. 13). Fragmentary assay data was available and digitised but has not been used in this study. Structural measurements were imported as delivered by EMX Royalty, who extracted these from their oriented cores drilled during their 2019 campaign. Subsequently, all the different lithologies that were logged and described by many geologists throughout the years, were grouped in six main groups: volcanic rock, magnetite ore, hematite ore, skarn, limestone, and sulfide ore (Figs. 13 and 14).

Table 3. Drill data used for 3D geological modelling in this study. Note that the model of Källfallsgruvan was based on mine maps compiled by Spahic (2021).

Model	Number of drillholes (n)	Total drill length (m)	Median drill length (m)	Maximum drill length (m)	Years of drilling
Total – from surface	336 67	43,735 15,127	104 207	671	1935–2019
Korphyttefältet-Bastnäsfältet	71	10,323	111	576	1979–2019
Persgruvan-Lerklockan	49	6,200	123	395	1958–2019
Källfallsgruvan	-	-	-	-	-
Pellegruvan-Bäckegruvan-Östergruvan	177	19,167	98	577	1958–2019
Svavelberget	34	7,684	203	671	1935–2019

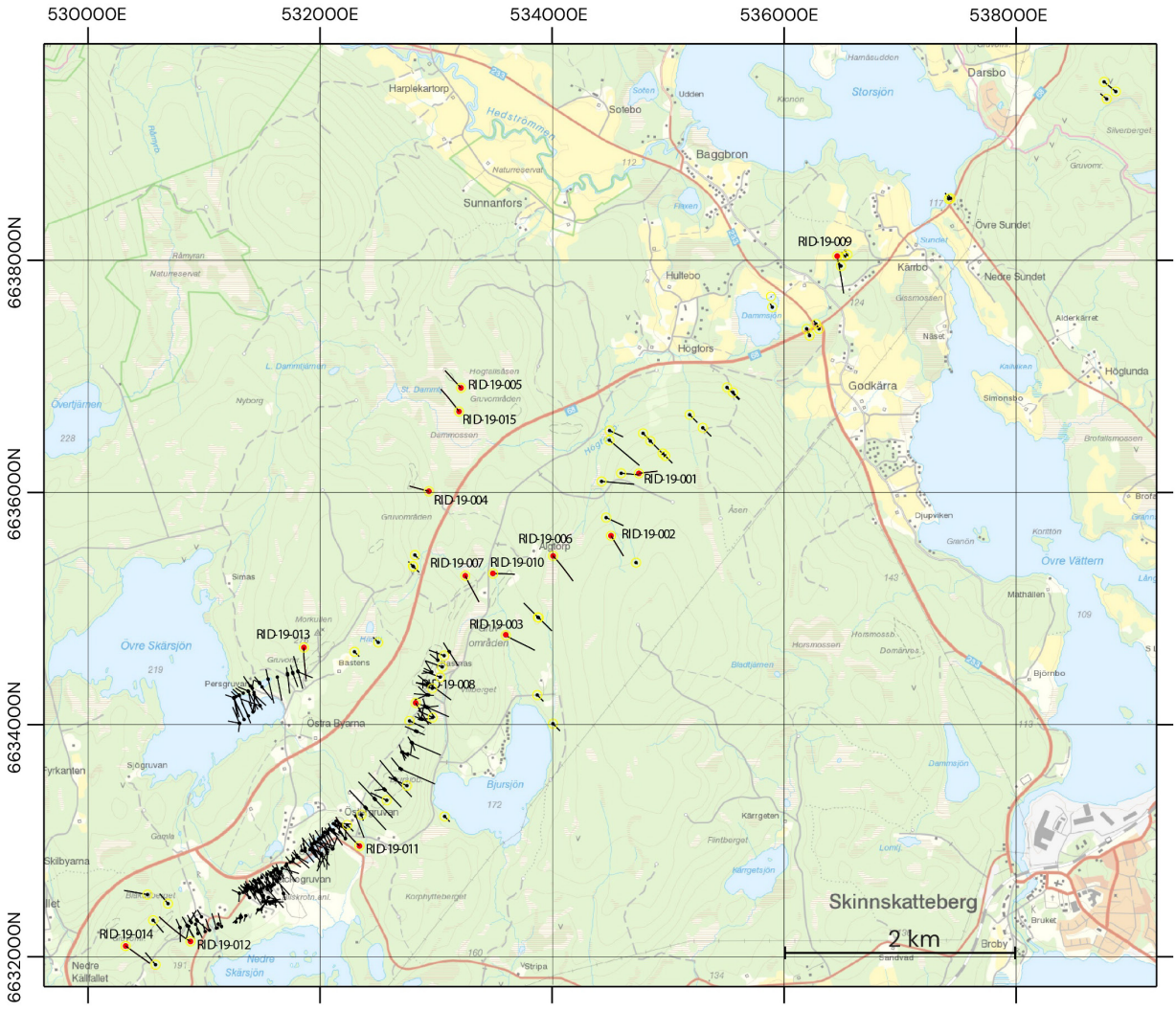

Figure 12. Map showing the locations of drillholes used for this study. Yellow halos mark the holes drilled from the surface. Red dots and labels refer to the exploration holes drilled by EMX in 2019.

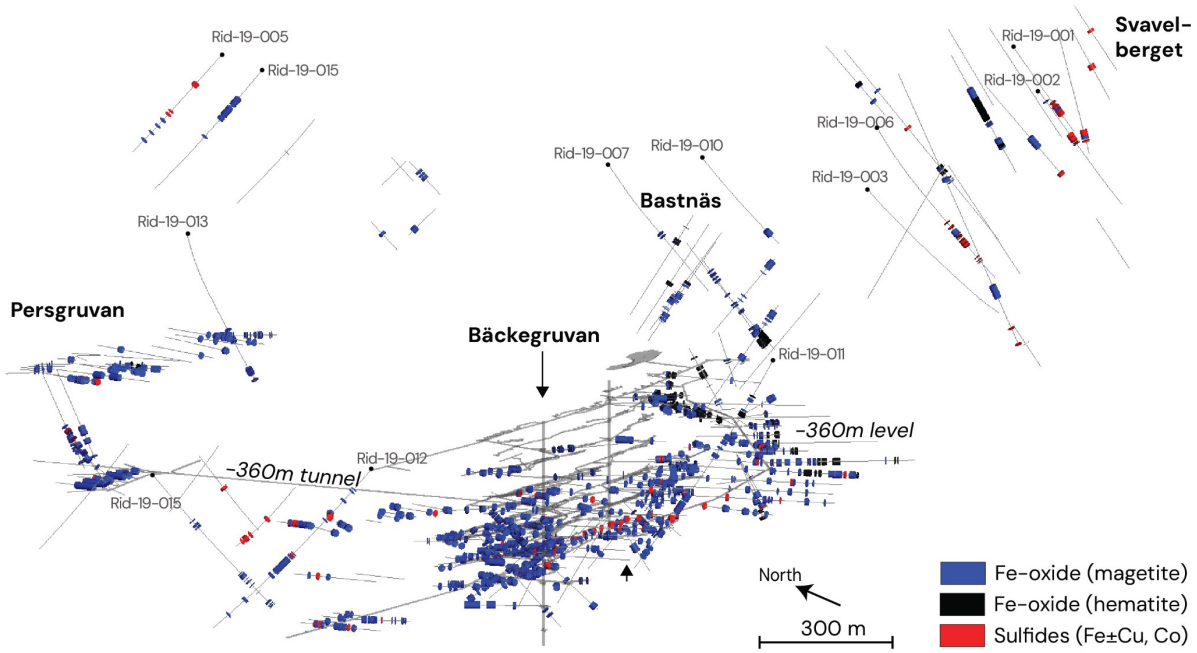

Figure 13. Drill traces and mineralised intervals shown in a 3D scene view in Leapfrog Geo.

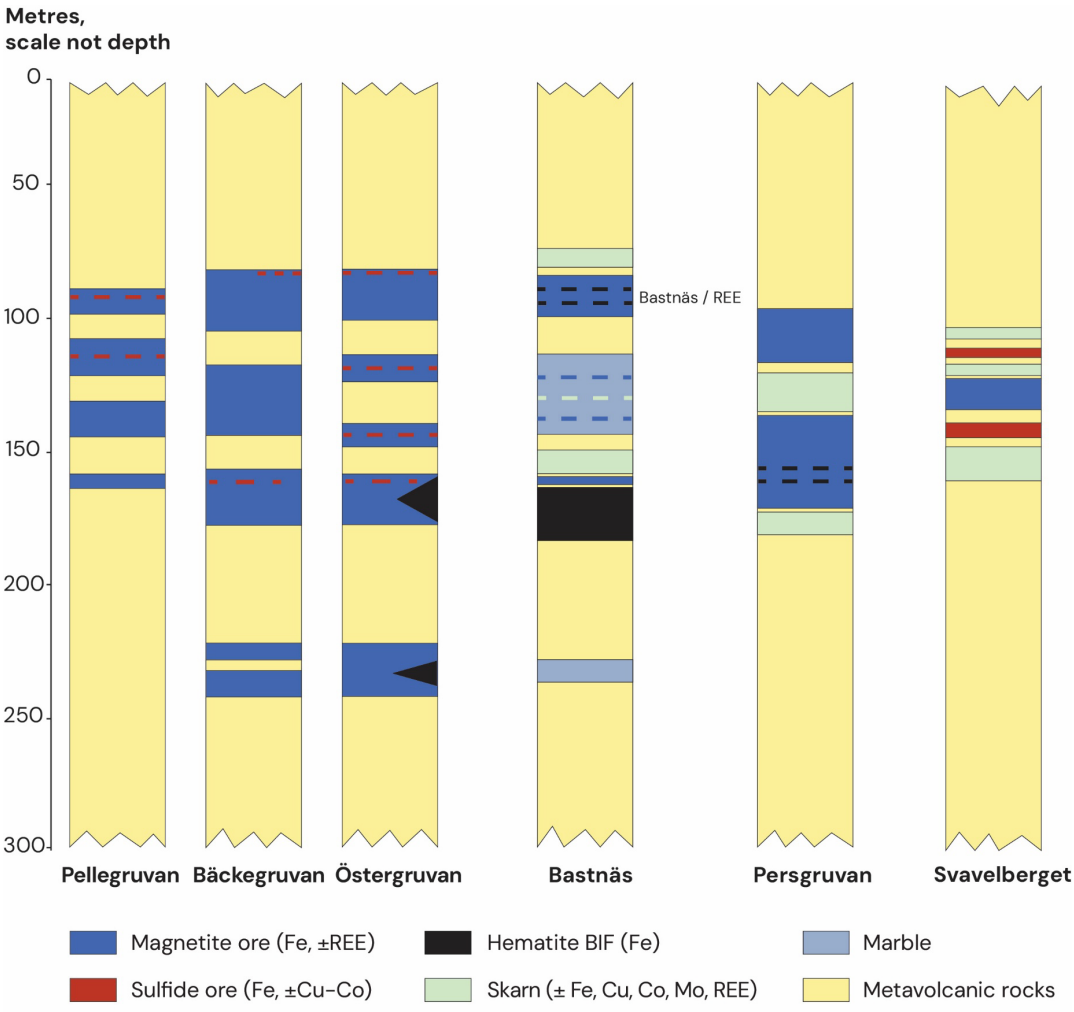

Figure 14. Simplified lithological columns based on representative drill cores for each of the modelled deposits. Hydrothermally altered rocks are not visualised here separately but do occur below, above and between the mineralised zones.

Mine level maps

Historic mine level maps have been used for the construction of most of the 3D geological models, apart from Svavelberget (Table 4, Fig. 15). Most maps show the outline of the different rock- and mineralisation types as well as the underground infrastructure and drill traces at a certain underground horizontal level. Their scale is either 1:800 or 1:1000. Vertical length- and cross-sections also exist for most mines, of which only some have been used in this study.

The mine maps were georeferenced into the coordinate system SWEREF 99TM and imported into Leapfrog Geo where they were vertically translated to their correct level. Subsequent tracing of the mapped contacts was done directly in Leapfrog Geo. The resulting polylines were used to model the outline of 3D orebodies in the case of closed polylines, or in the case of open polylines, to constrain the geometry of the footwalls or hanging walls of veins. The underground infrastructure is also based on mine maps and has been digitised by EMX Royalty.

The ore bodies of the Källfallsgruvan geological model are solely based on mine maps and were constructed in SKUA-GOCAD by Edna Spahic (2021). She created closed polylines outlining the main ore on each mine level map, which were then combined to create a single closed surface representing the ore body. Here, the resulting surface was imported as a mesh into Leapfrog Geo.

Table 4. Mine level maps used for 3D geological modelling in this study.

Model	Mine maps (n)	Map scale	Deepest level, mining (m)	Deepest level, tunnel (m)	Reference
Korphyttefältet–Bastnäsfältet	8	1:1000	-115	-360	Mannerstråle (1886-1910)
Persgruvan–	6	1:800	-145	-360	Malmgren (1910-1984)
Lerklockan	4	1:800	-115	-180	Hedberg (1897-1923) Bergquist (1985)
Källfallsgruvan	7	1:800	-300	-	Sundholm (1899-1971)
Pellegruvan–	6	1:1000	-175	-360	Fredriksson (1932-1984)
Bäckegruvan–	9	1:1000	-310	-360	Bergquist (1982-1985)
Östergruvan	9	1:1000	-310	-360	Mörtsell (1921-1957) Mörtsell (1927-1953)
Svavelberget	-		-		-

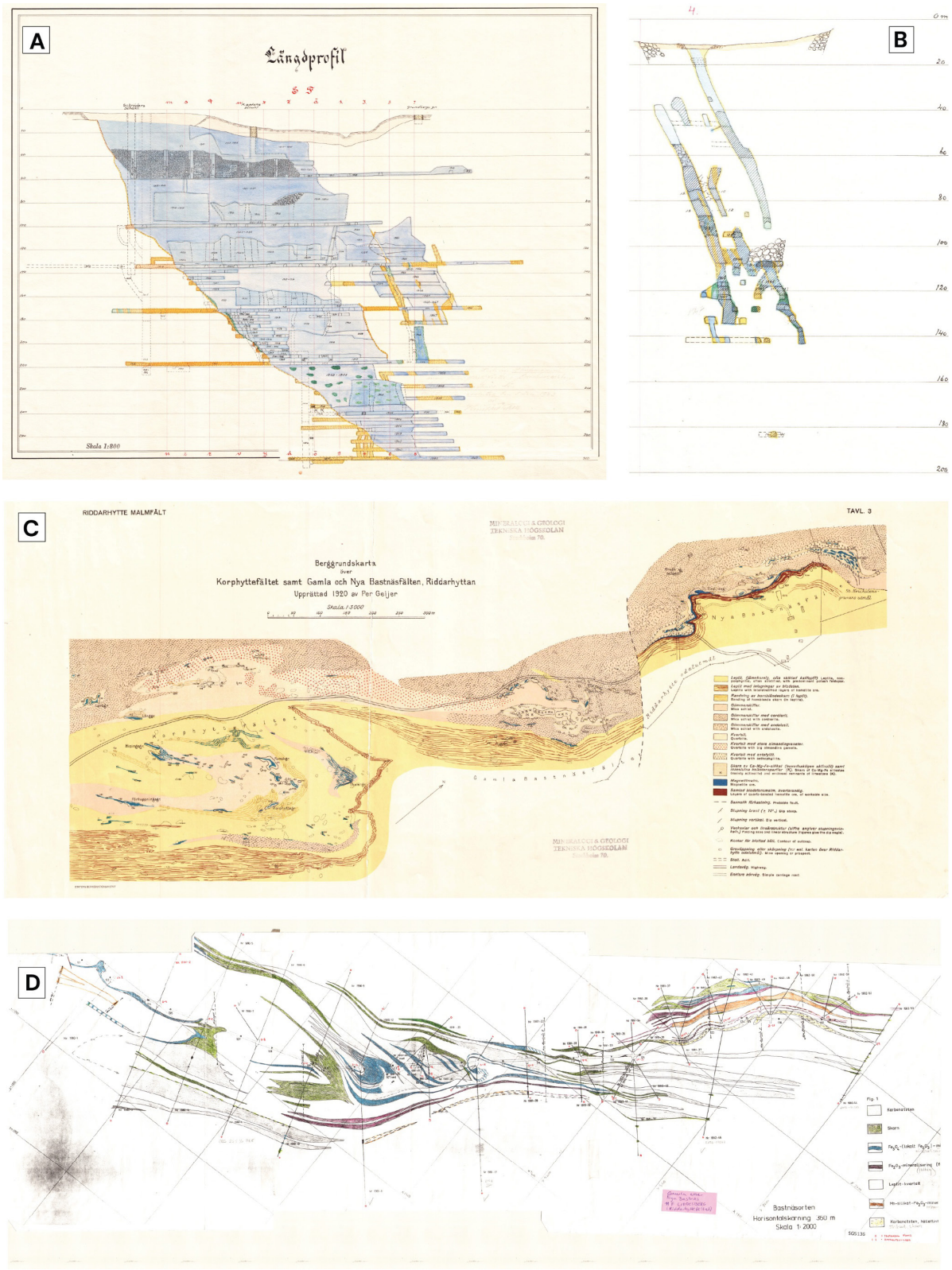

Figure 15. A selection of mine level maps, cross-sections and historical surface maps used for 3D geological modelling. **A–B.** Length- and cross-section through Källfallsgruvan. **C.** Geological map of the Korphyttefält and Bastnäs by Geijer (1921). **D.** Mine level map (-360m level) based on the Bastnäs exploration tunnel.

Modelling results

Factsheets are presented to provide a fast overview of the results for each model (Figs. 16 to 23). The sheets include overview maps, 3D views and short summaries on model dimensions, input data, overall structure and output volumes. More model specific information on the modelling results, uncertainty, and emphasis on certain local and regional features is written below for each model. A discussion on the interpretation of the modelled features and their geological significance is presented in the following chapter *Discussion*.

A short video that shows all the models presented below can be seen here:
https://play.mediaflow.com/ovp/16/43PE9PKLS1

Korphyttefältet–Bastnäs

The Korphyttefältet–Bastnäs model builds heavily on earlier interpretations from Ihre & Sädbom (1986), who sketched Korphyttefältet as a refolded fold, or more specifically an S-folded Z-fold. These authors in turn based their model on stratigraphic way-up indicators interpreted from outcrops, which were not further evaluated during this study. Their suggested model, now combined with drill data, structural data, mine-level maps and magnetic anomaly maps, appears still valid and is considered the most likely model in three dimensions (Fig. 16). In contrast, between Korphyttefältet and Bastnäsfältet we interpreted from the magnetic anomaly map a NE-striking shear zone that dismembers the main synform in a dextral sense. As such, the stratigraphic sequence at Bastnäs resembles that of Korphyttefältet but is structurally located in the opposing and overturned fold limb. The model is well constrained between the surface and the exploration tunnel at the -360 m level. Below that and down to 700-meters depth, the model is very poorly constrained. Here, the preservation of a sub-vertically dipping sequence is only presumed and extrapolated from the upper part of the model.

A short video of the Korphyttefältet–Bastnäs model can be seen here:
https://play.mediaflow.com/ovp/16/33PENP2LB1

Persgruvan–Lerklockan

The orebodies at Persgruvan and Lerklockan have been modelled as a series of lenses (Fig. 17). These lenses resemble two parallel ore layers striking northeast and dipping steeply towards the northwest. Slightly shallower dips (c. 70–60°) are modelled between the -145 m and the -360 m level. The ore layers are strongly boudinaged, resulting in local thinning in the necks and thickening in the swell, or in the extreme case into isolated megaboudins. The 3D geometry of the lenses (megaboudins) was constrained by mine-maps, drill data and structural measurements and was modelled in Leapfrog Geo by the vein-modelling tool. The resulting geometries of the megaboudins are oblate (pancake-shaped) to somewhat prolate (cigar-shaped). Their long axes align with the measured stretching lineations. A fault plane divides the model into two blocks and accommodates approximately 40 meters dextral displacement between the ore layers on both sides.

A short video of the Persgruvan–Lerklockan model can be seen here:
https://play.mediaflow.com/ovp/16/44PEYPRL91

Pellegruvan–Bäckegruvan–Östergruvan

This model combines the Fe-Cu-Co ore bodies of Pellegruvan, Bäckegruvan and Östergruvan into a single model (Fig. 18). All deposits are part of a network of three to five ore layers which strike northeast and dip mainly (sub)vertically. Local intersections, pinch-outs and slight variations in strike and dip of individual layers, however, give an anastomosing appearance when viewed horizontally or vertically. The ore layers were modelled in Leapfrog as a vein-network constrained by map traces from the magnetic anomaly map, and at deeper levels from mine level maps, drill data and structural data from oriented drill core. Particularly at Bäckegruvan and Östergruvan, densely spaced drilling resulted in a rather well constrained model, which reveals a significant volume of unmined Fe-Cu-Co ore that most likely continues at depth beyond the model space (>550 m).

A short video of the Pellegruvan–Bäckegruvan–Östergruvan model can be seen here: https://play.mediaflow.com/ovp/16/25PEJPRL92

Källfallsgruvan

The 3D orebody of Källfallsgruvan includes massive magnetite mineralisation (~62% Fe) and semi-massive/disseminated magnetite mineralisation (~45% Fe) (see also Spahic 2021). The mineralisation extends to a depth of approximately 300 meter below ground surface level and dips steeply towards the southwest (Fig. 19). The overall ore body geometry mimics an S-shaped, steeply plunging synform, which tightens towards deeper levels (Spahic 2021). On a semi-regional scale, the mineralisation occurs on the refolded limb of a Z-fold, which in turn represents a drag fold of a northeast-striking magnetite-skarn layer. The layer dips between subvertical and 70° towards the southeast. Modelling of the magnetite-skarn layer was done in Leapfrog as a Structural Surface using constraints from structural measurements and the magnetic anomaly map. Thicknesses are solely based on surface data and vary between 10 meters along the long fold limb to 30 meters in the short limbs and fold hinge zones.

A short video of the Källfallsgruvan model can be seen here: https://play.mediaflow.com/ovp/16/60PE3PDLG1

Svavelberget

The 3D model of the massive sulfide mineralisation of Svavelberget reveals three NE-striking, rather straight vein segments (Fig. 20). All veins are truncated and displaced by a vertical NNE-striking fault. The northern segment is constrained by mineralised intervals from four legacy bore holes. Hole RID-19-009, drilled by EMX Royalty in 2019, also intersects the northern vein but no mineralisation was found, which may suggest some local disruption and pinch outs of the northern vein. The southern vein segment is constrained by more drill holes that are evenly distributed along strike. In contrast to its northern equivalent, the southern vein continues west of the modelled fault but pinches out just north of Bastnäs.

Skräppbo synform

The name "Skräppbo" is used here for the area that includes among others the iron-mineralisations of Skärsjöfältet, Norra Skilåfältet and Norra Blankagruvan. The Skräppbo synform has been modelled here as a doubly plunging synform with two opposingly trending hinge zones (Fig. 21). The synform is broken into three parts by two cross-cutting faults that accommodated both horizontal and vertical displacements. The bulk of the Skräppbo synform strikes NW, but the westernmost part of the fold strongly bends towards the south into a pointy

hook-shape. Iron mineralisation is restricted to the fold's southern limb, which is in turn strongly refolded by steeply plunging S- and Z-folds. Magnetite-skarn layers have been modelled as three separate veins, but presumably all belong to the same stratigraphic horizon. The structure is primarily based on map traces interpreted from the magnetic anomaly map, new structural measurements as well as from the SGU bedrock map (Ambros, 1983a). Drill data in this part of the study area is entirely absent.

Regional fault–block model

The regional fault-block model includes 20 faults which divide the model space into 30 separate fault blocks (Fig. 22). The bulk of the faults were derived from the geophysical lineament map (Fig. 8) and modelled as surfaces by vertical extrapolation of the horizontal traces. Hereby it is assumed that all the faults are dipping vertically. A continuous northern and a southern boundary fault confines the central part of the model, which largely coincides with the sedimentary-volcanic rock domain. Both boundary faults strike NE to ENE, respectively. The central domain is made up of relatively small fault blocks that are bounded by a dense network of NW- and partly curved NE-striking faults. We interpret this structure as a strike-slip duplex. Sinistral slip along these NE-striking faults are inferred from the local displacements of NW-striking faults.

Regional structural framework

The regional structural framework is a continuation of the fault-block model and includes also structural surfaces to portray the folding pattern, and all the modelled ore bodies. A resulting striking feature is the inferred interplay between folds and faults, which suggests both sinistral and dextral shearing. As such, the ore bodies from Pelle- Bäcke- and Östergruvan appear to connect with the orebodies of Persgruvan–Lerklockan through what we refer to as the Central synform. From this model we even postulate that all of the iron mineralisation in the region occurs on the same stratigraphic level, which initially may have been a continuous layer (See chapter *Discussion).*

Korphyttefältet–Bastnäsfältet

Object

Korphyttefältet and Bastnäsfältet (northern part) were mined until the 1920's for iron, copper, cerium (Ceritgruvan) and marble. The mineral occurrences are described in Söderhielm et al. (2023).

Modelling

Model dimension: 1,200 m × 800 m × 500 m.
Model input: 71 drillholes with total length of 10,323 m, exploration tunnel, structural measurements, mine maps and bedrock and magnetic anomaly map. **Tools**: Leapfrog Geo: *Vein-modelling* and *Structural surfaces*

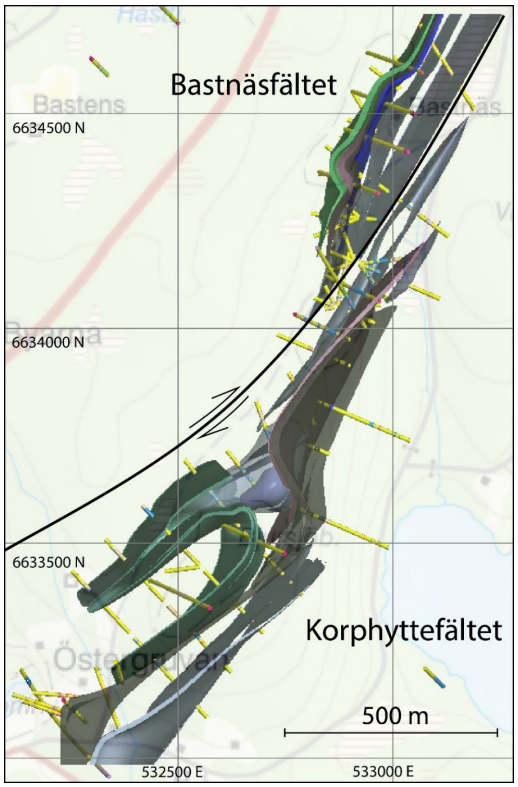

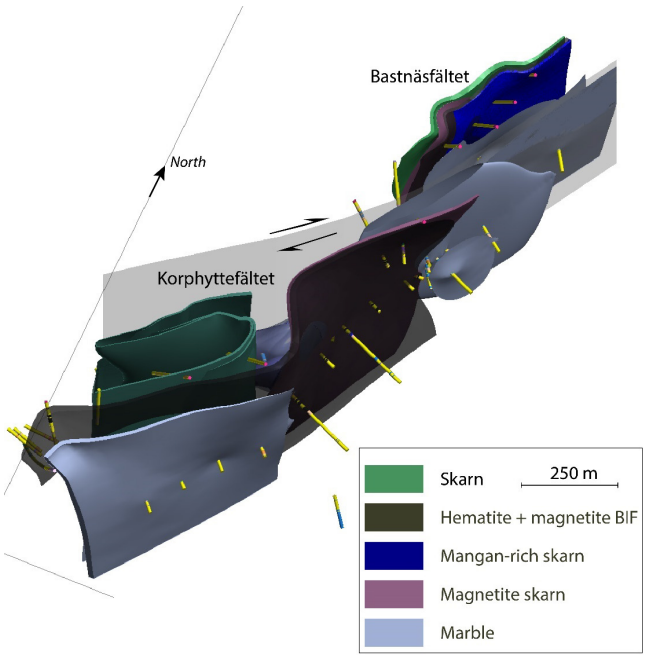

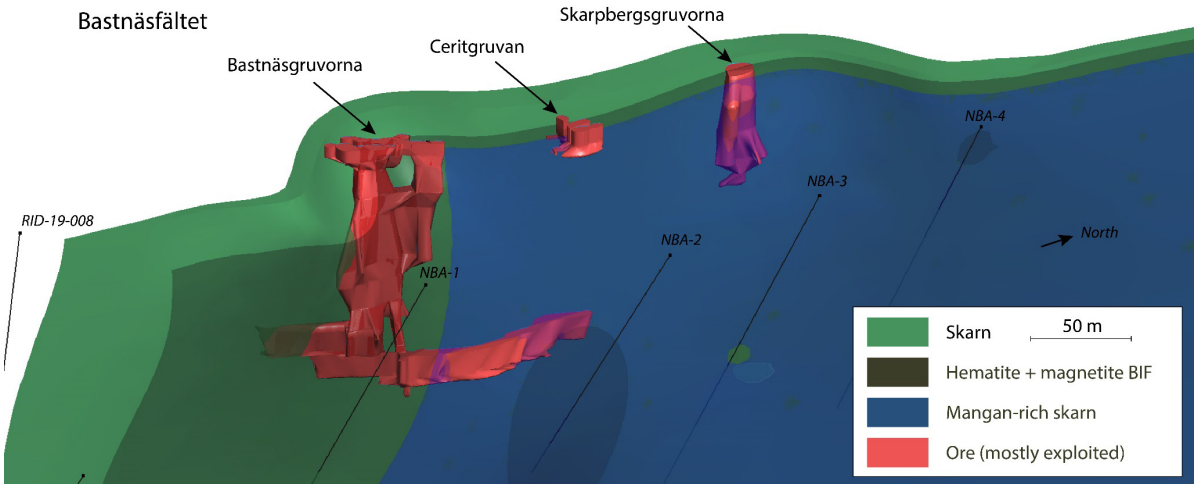

Structure

Korphyttefältet is modelled as an S-folded Z-fold. A shear zone follows the central marble and marks the border between the Korphyttefältet to the south and the Bastnäsfältet to the north.

Modelled volumes

Hematite-magnetite BIF: 18,732,000 m^3, Magnetite skarn: 3,399,000 m^3, Mangan skarn: 2,435,700 m^3, Extracted volume: 77,270 m^3

Figure 16. 3D model factsheet on Korphyttefältet.

Persgruvan–Lerklockan

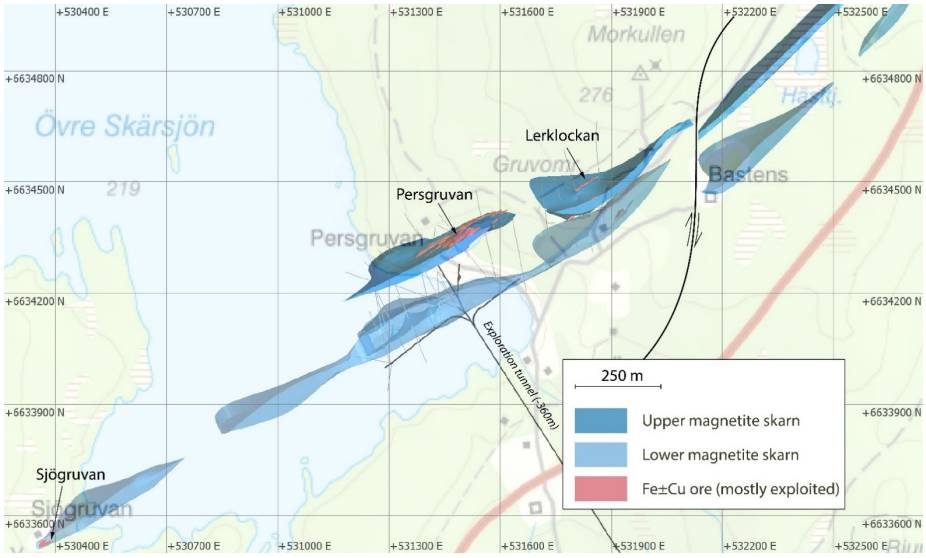

Object

Persgruvan and Lerklockan were mined until 1967 for iron and copper. The mineral occurrences are described in Söderhielm et al. (2023).

Modelling

Model dimension: 3,000 m × 2,080 m × 600 m.
Model input: 49 drillholes with total length of 6,200 m, structural measurements, mine maps and magnetic anomaly map.
Tools: Leapfrog Geo: *Vein-modelling*

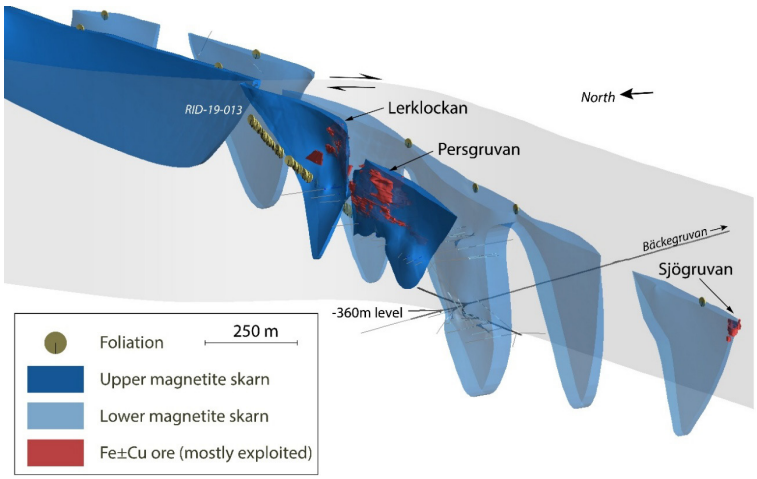

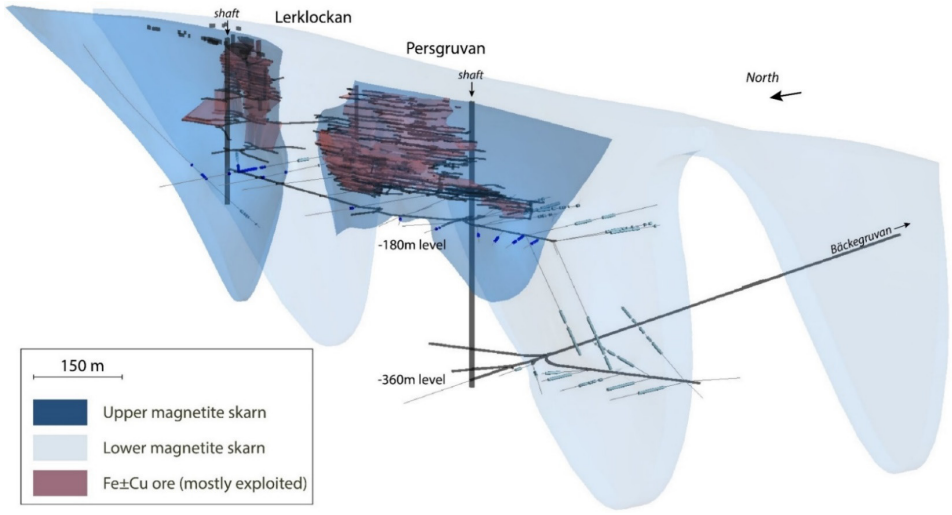

Structure

Two boudinaged magnetite-skarn layers dipping steeply towards the northwest.

Modelled volumes

Magnetite skarn: 34,196.300 m^3
Extracted volume: 494,190 m^3 (period 1880–1967)

Figure 17. 3D model factsheet on Persgruvan-Lerklockan.

Pellegruvan–Bäckegruvan–Östergruvan

Object

Pellegruvan, Bäckegruvan and Östergruvan were mined for copper and iron until 1979 (Bäckegruvan). Mineralisations are described in Söderhielm et al. (2023). Most recent drilling by EMX Royalty in 2019.

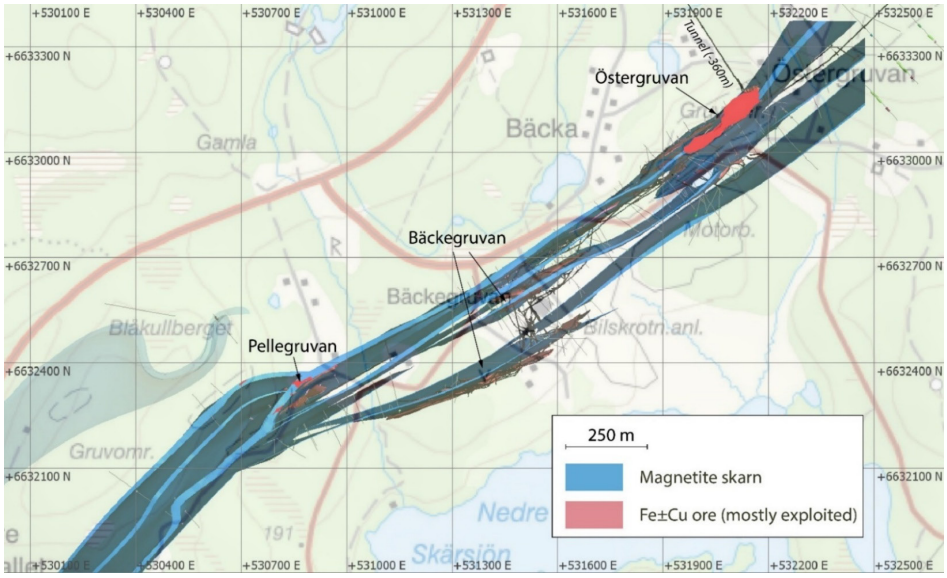

Modelling

Model dimension: 2,600 m × 1,900 m × 550 m. **Model input:** 177 drillholes, total length 19,167 m, structural data, mine maps and magnetic anomaly maps. **Tools:** Leapfrog Geo: *Vein-modelling*

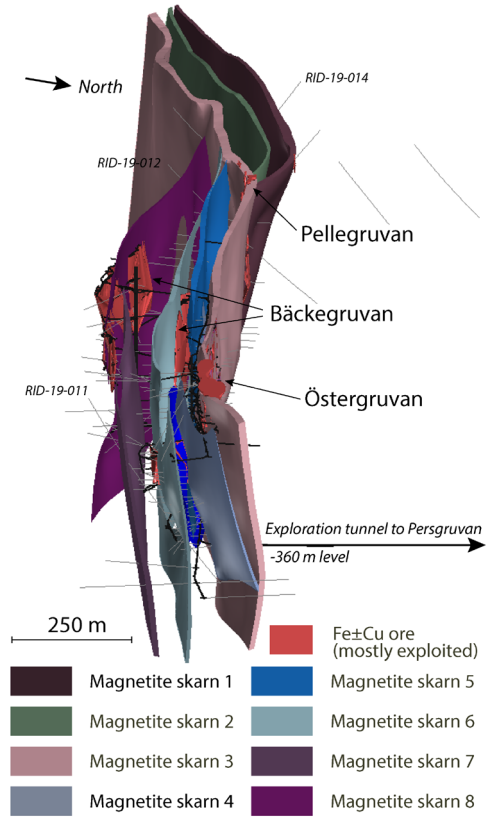

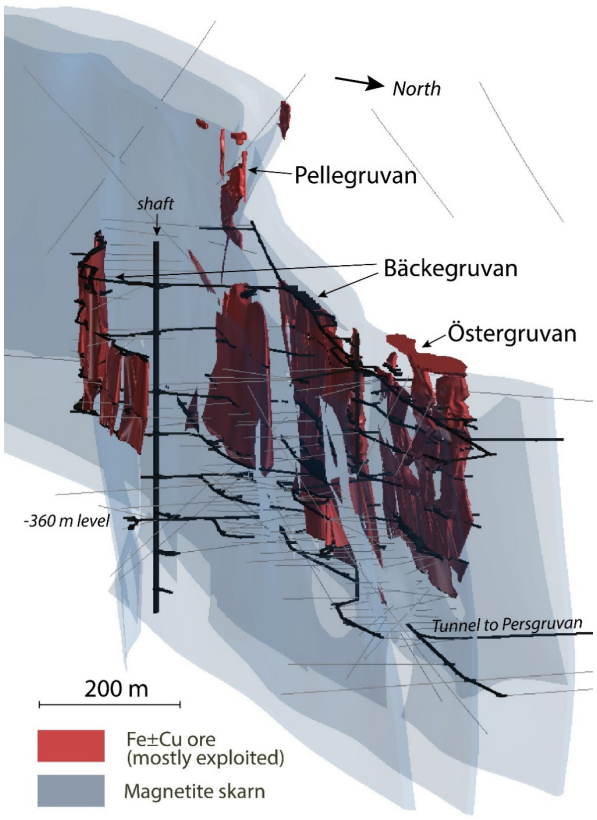

Structure

NE-striking network of eight magnetite layers.

Modelled volumes

Magnetite skarn: 43,959,000m^3. Extracted: 790,803 m^3

Figure 18. 3D model factsheet on Pellegruvan – Bäckegruvan – Östergruvan.

Källfallsgruvan

Object

Källfallsgruvan was mined until 1967 for magnetite (c. 62% Fe). See Spahic (2021) and Söderhielm (2023).

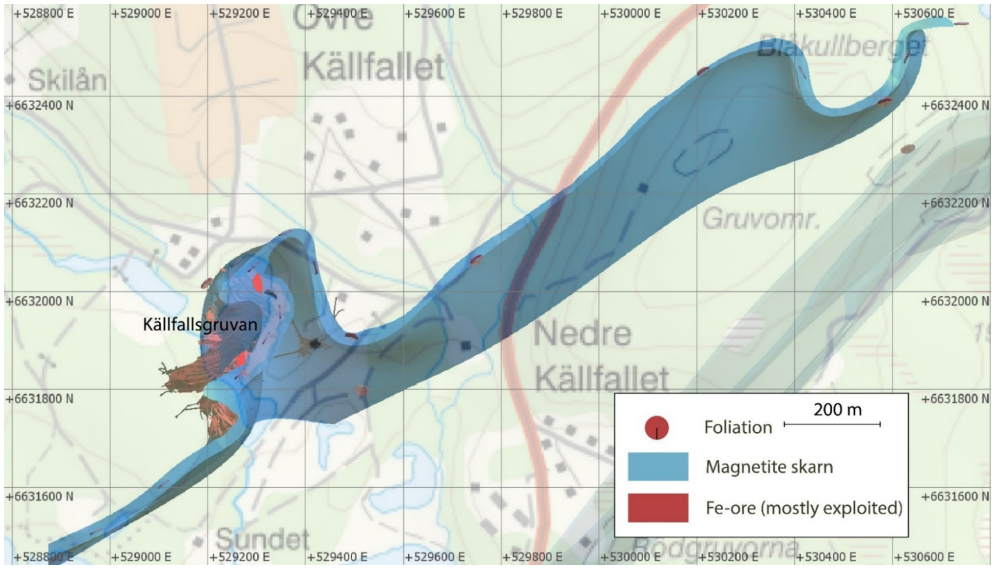

Modelling

Model dimension: 2,000 m × 1,200 m × 500 m. **Model input:** Structural measurements, mine maps and magnetic anomaly maps. **Tools:** SKUA-GOCAD for the ore body, Leapfrog Geo: *Vein-modelling*

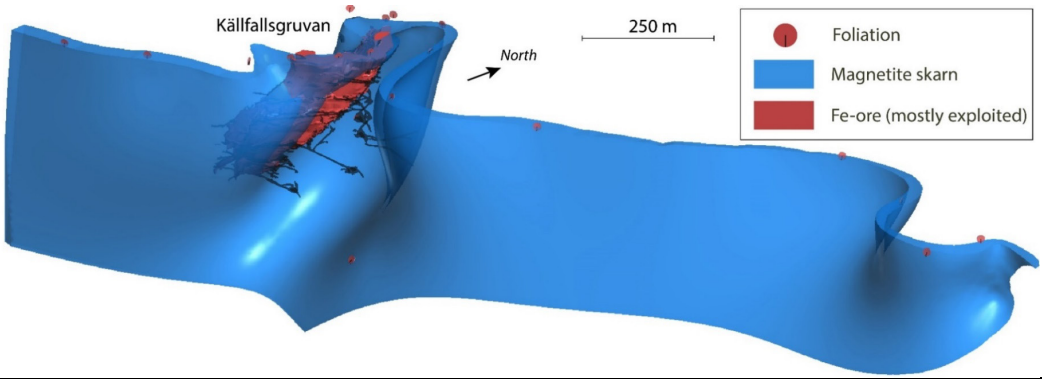

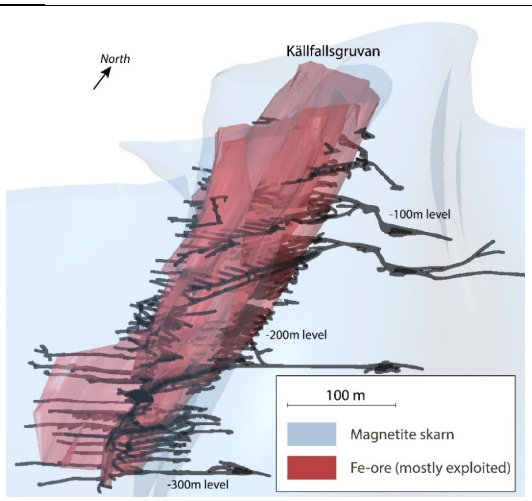

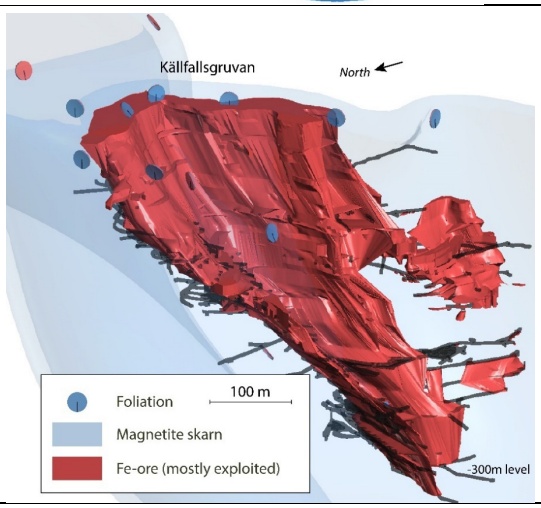

Structure

Steeply SW-plunging S-fold.

Modelled volumes

Magnetite skarn: 13,902,000m^3. Extracted: 1,058,800m^3

Figure 19. 3D model factsheet on Källfallsgruvan.

Svavelberget

Object

Discordant, NE-striking veins of massive sulfide mineralisation that intersect the regional folding trend. Mineralisation consists mainly of pyrrhotite and has been extensively drilled by EMX Royalty in 2019.

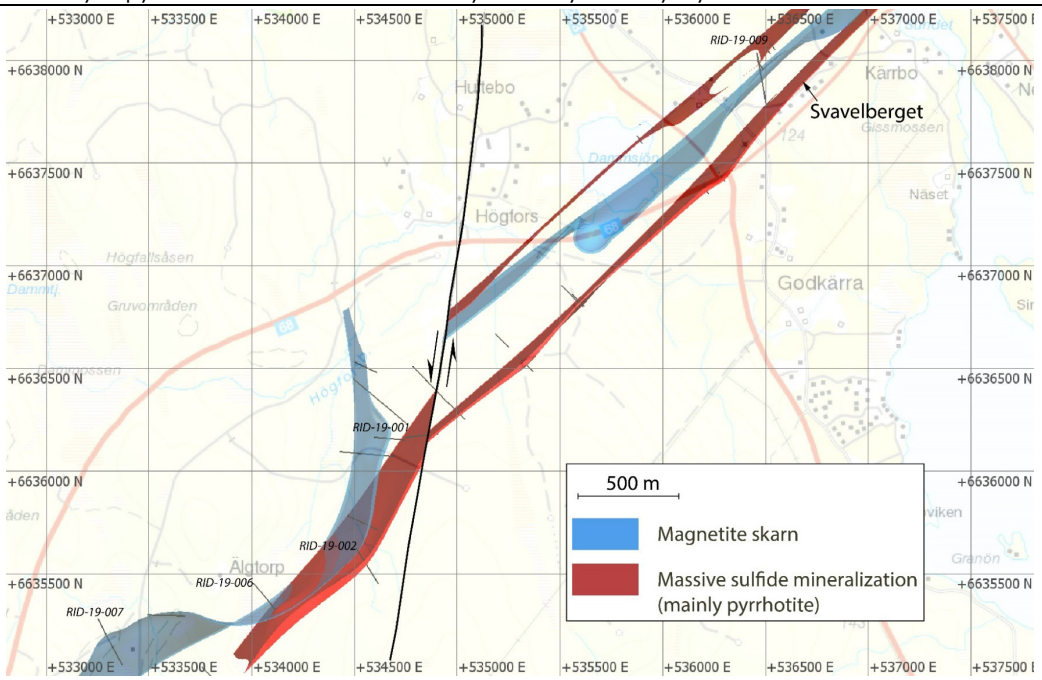

Modelling

Model dimension: 4,500 m × 4,000 m × 700 m. **Model input:** 34 drillholes, total length 7,684 m and magnetic anomaly maps. **Tools:** Leapfrog Geo *Vein-modelling*

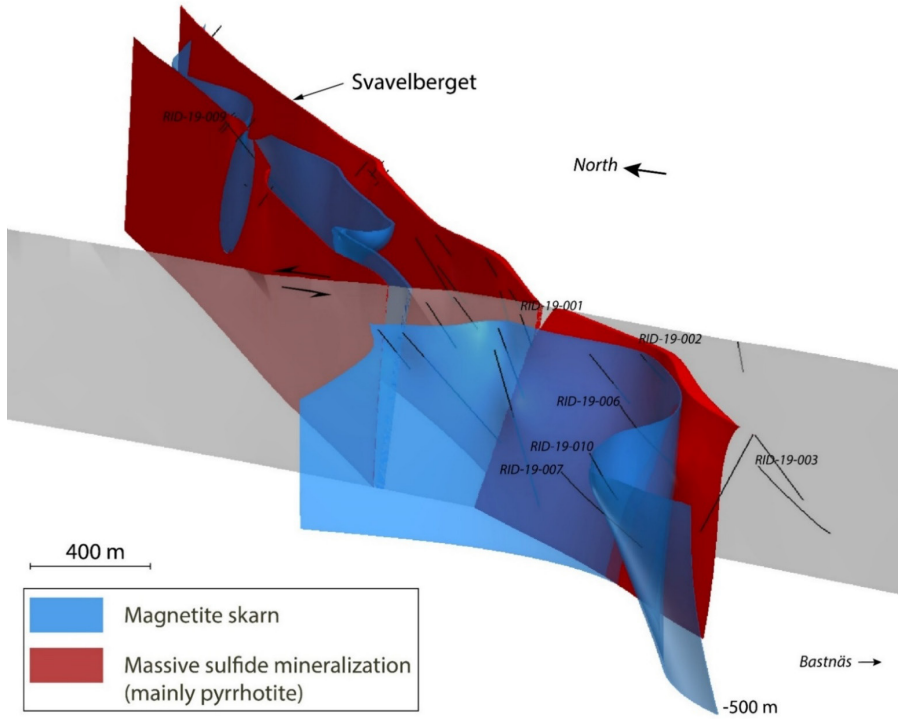

Structure

Two parallel NE-striking sulfide veins.

Modelled volumes

Massive sulfide: 48,487,800 m^3. Magnetite skarn: 53,336,000 m^3

Figure 20. 3D model factsheet on Svavelberget.

Skräppbo Synform

Object

The Skräppbo synform is a regional-scale fold that is doubly plunging with its deepest keel below the central part. The fold is refolded and faulted. Magnetite skarn and iron mineralisations occur along the southern fold limb.

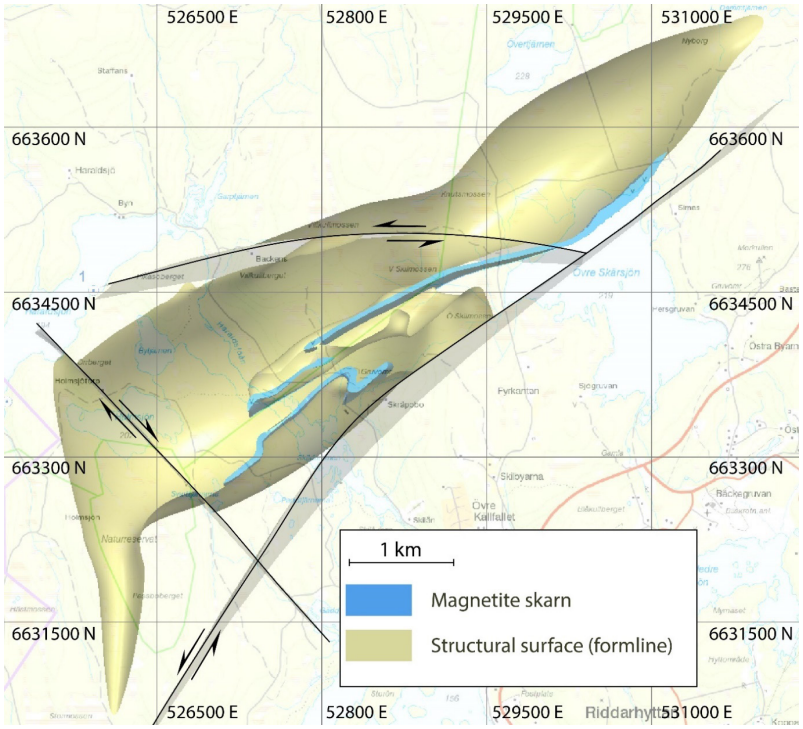

Modelling

Model dimension: 7.5 × 5.8 × 0.6 km
Model input: Structural measurements, magnetic anomaly map, SGU bedrock map and mineral database.
Tools: Leapfrog Geo, *Vein-modelling* combined with *Structural modelling*.

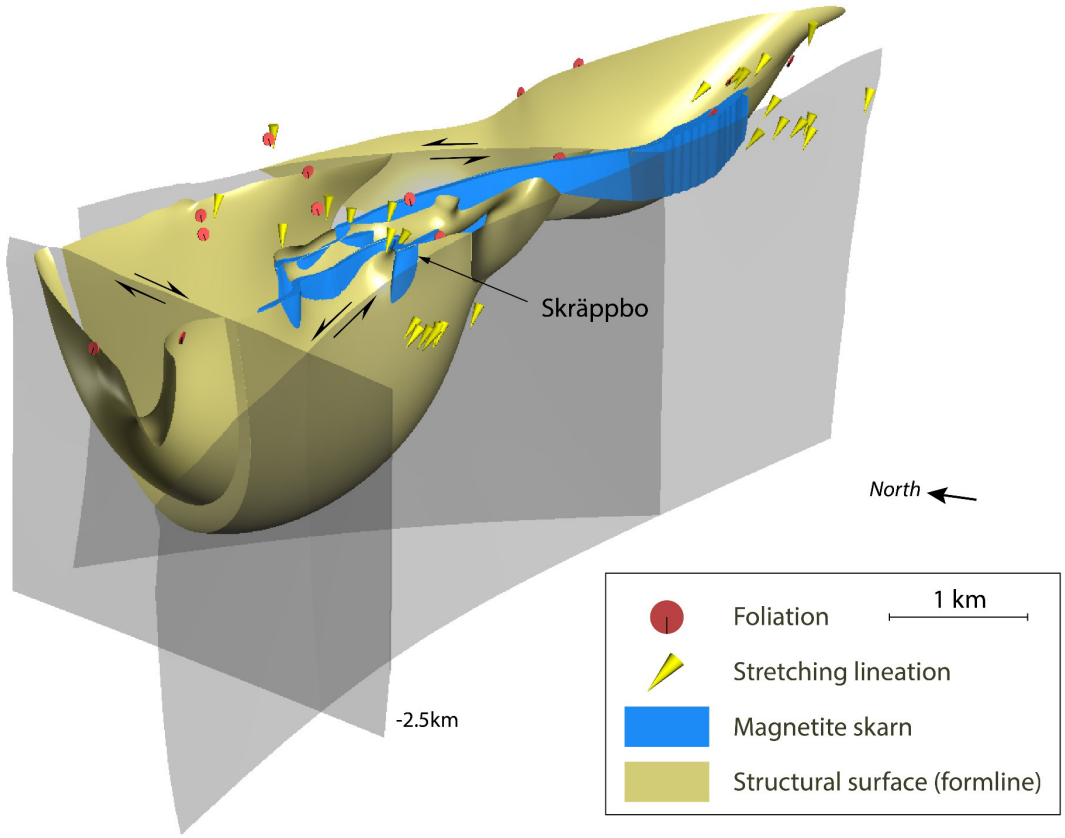

Structure

Refolded and faulted doubly-plunging synform.

Modelled volumes

Magnetite skarn (low grade): 156,385,000 m^3. No extraction

Figure 21. 3D model factsheet on the Skräppbo synform.

Regional fault-block model

Object

Riddarhyttan Ore Field within its regional context.

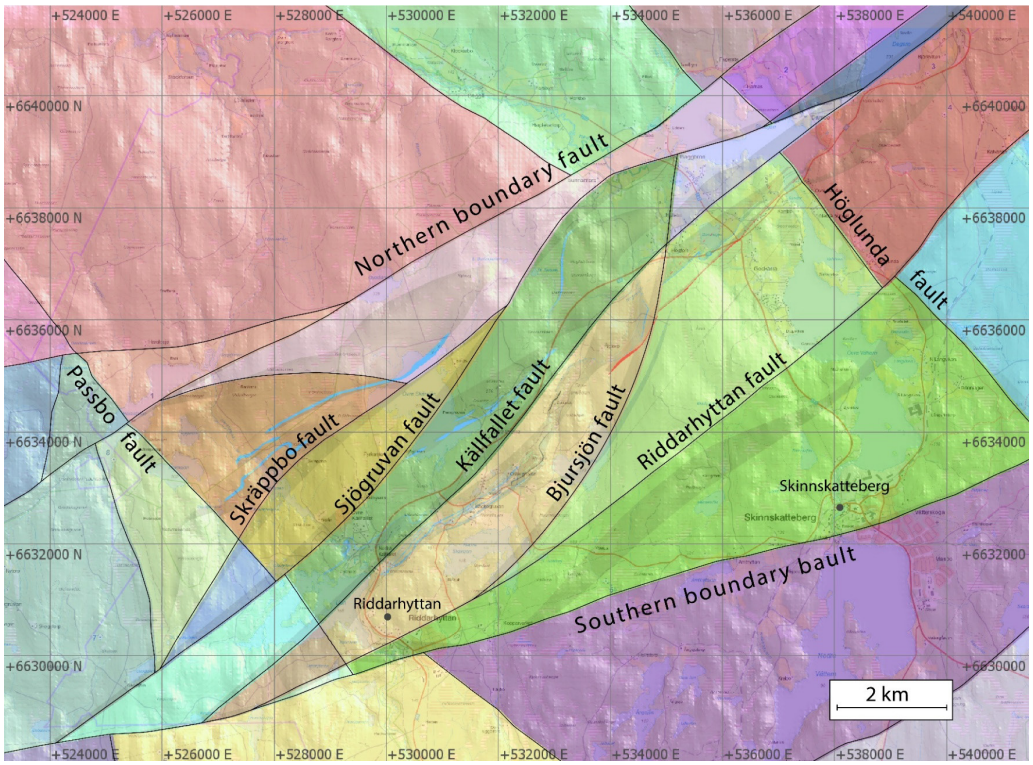

Modelling

Model dimension: 19 km × 15 km × 3 km. **Model input:** Lineaments from magnetic anomaly maps.
Tools: Leapfrog Geo: *Faulted geological model*

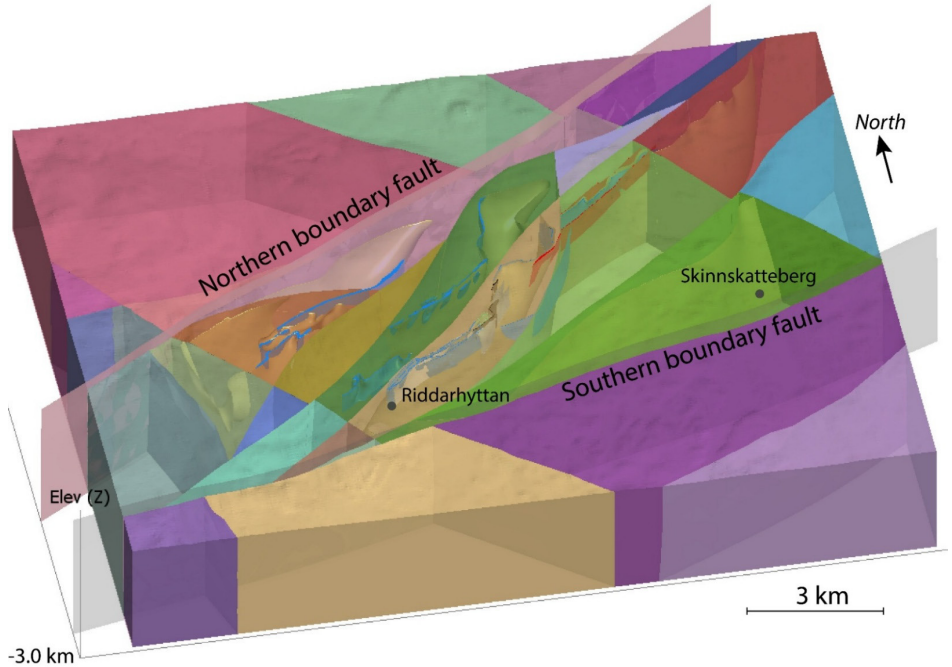

Structure

Strike-slip duplex between two boundary faults

Modelled elements

20 faults and 30 fault blocks

Figure 22. Factsheet of the regional fault block model.

Regional structural framework

Object

Local deposit models of the Riddarhyttan Ore Field within a regional context.

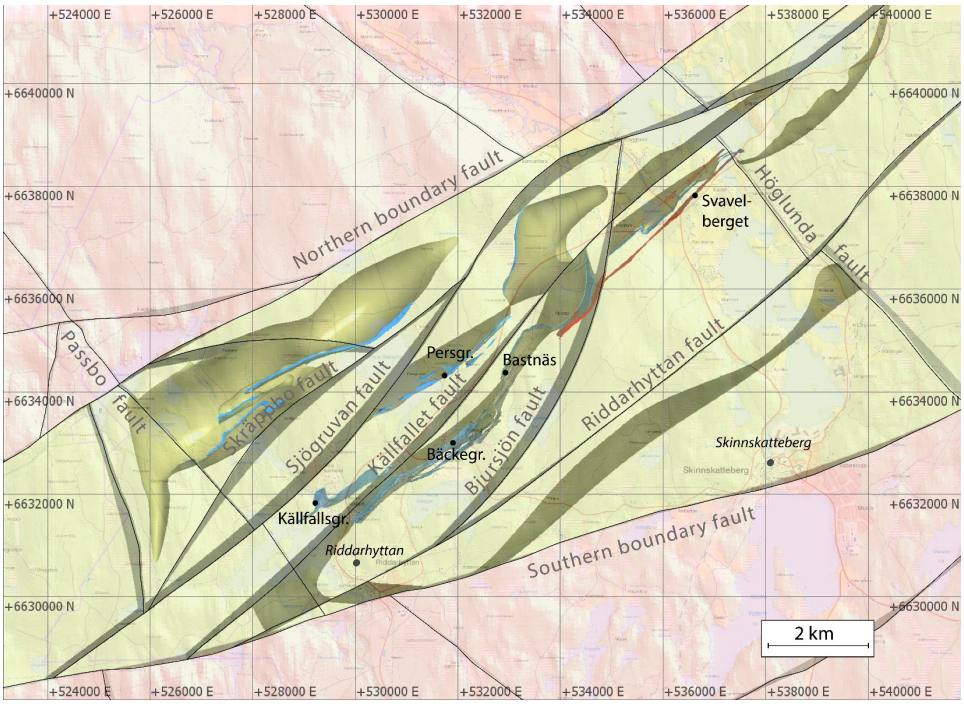

Modelling

Model dimension: 19 km × 15 km × 3 km. **Model input:** Structural measurements, bedrock- and magnetic anomaly maps and six static deposit models. **Tools:** Leapfrog Geo: *Structural surfaces*

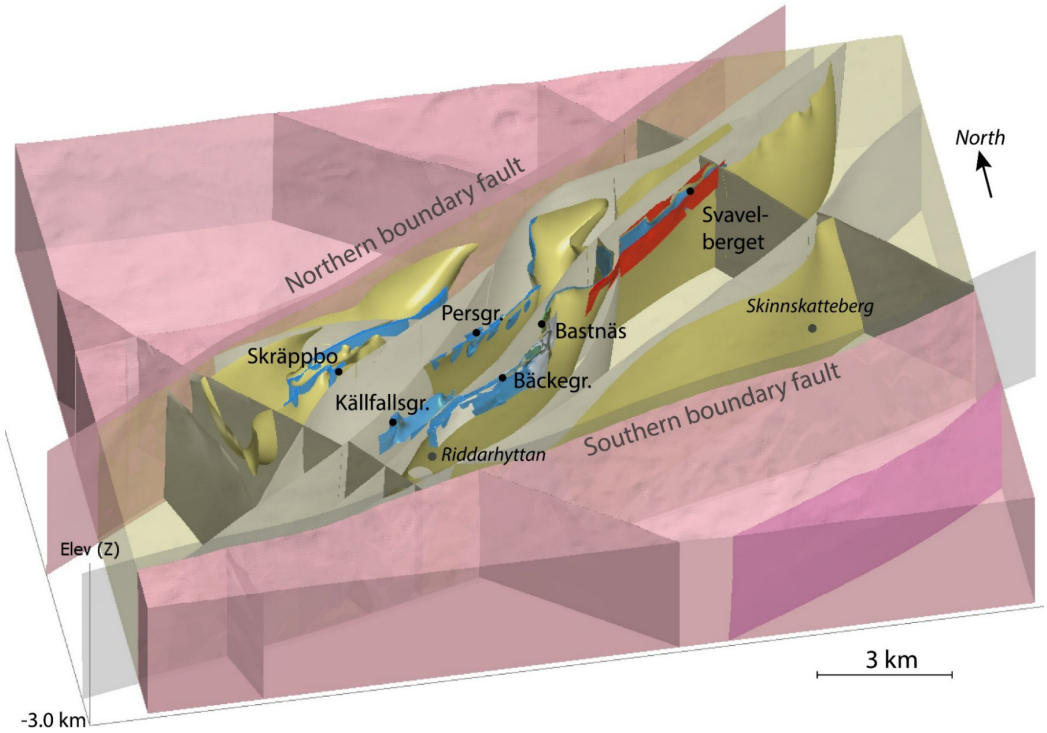

Structure

Strike-slip duplex between two boundary faults.

Modelled elements

20 faults, 10 structural surfaces, 6 deposit models.

Figure 23. Factsheet of the regional structural framework model.

Interpretation and discussion

Structural-geological map and cross-section

A new geological map and corresponding cross-section are presented in Figure 24. Both are synchronised with the obtained results from 3D modelling, new interpretations of the magnetic- and electromagnetic anomaly maps, and the pre-existing bedrock map by Ambros (1983a). The mineralisation outline, form-lines and fold traces are derived from the 3D modelling results presented in the previous chapter. Lineaments are interpreted from the most recent airborne magnetic and resistivity anomaly maps (Figs. 4–5 and 8). The lithological contacts are from the pre-existing bedrock map and are locally modified based on the 3D modelling results. The 2D-cross-section that coincides with the new map is based on drill data and structural measurements from this study, and a few way-up indicators from earlier studies. Below the drill depth of the c. -360 m level, the interpretation is purely conceptual and therefore uncertain.

The resulting map shows a series of large, sub-parallel synforms and antiforms (Fig. 24). Based on field evidence, these folds are clearly folding S_0 bedding and S_1 tectonic foliations and are therefore classified as F_2 folds. Within the central part of the area, these F_2 folds are slightly overturned and have fold-axes plunging 40° to 70° towards the southwest. Parasitic F_2 folds occur on the limbs of the larger folds and are generally S- or Z- asymmetric with steeply to vertically plunging fold axes. Large folds, like the Riddarhyttan antiform and the Skräppbo synform are doubly-plunging folds with fold axes plunging both towards the northwest and to the southeast. This doubly-plunging fold structure mimics an elongated dome geometry and may have resulted from sheath folding during oblique shearing, or alternatively and probably more likely, by re-folding of F_2 folds along NW–SE trending F_3 axial traces. Hence, we interpreted several F_3 folds from folded lithological contacts throughout the Riddarhyttan area (Fig. 24).

Many of the folds are disrupted by faults, along which displaced markers reveal both dextral and sinistral shearing. Most of the faults merge into the Northern and Southern boundary faults, outlining a so-called fault duplex. A duplex comprises multiple fault blocks that are imbricated and stacked onto each other. The overall asymmetry of this fault duplex suggests predominantly dextral shearing during its formation. As such, it showcases the interplay between progressive shearing and folding during D2 transpression. Moreover, we propose that the bulk of magnetite skarn and related mineralisation of Riddarhyttan occur within the same stratigraphic level, which is exposed at several places throughout the area due to folding and faulting. We continue the discussion on how the mapped structures may have formed by proposing a conceptual kinematic model in the following section.

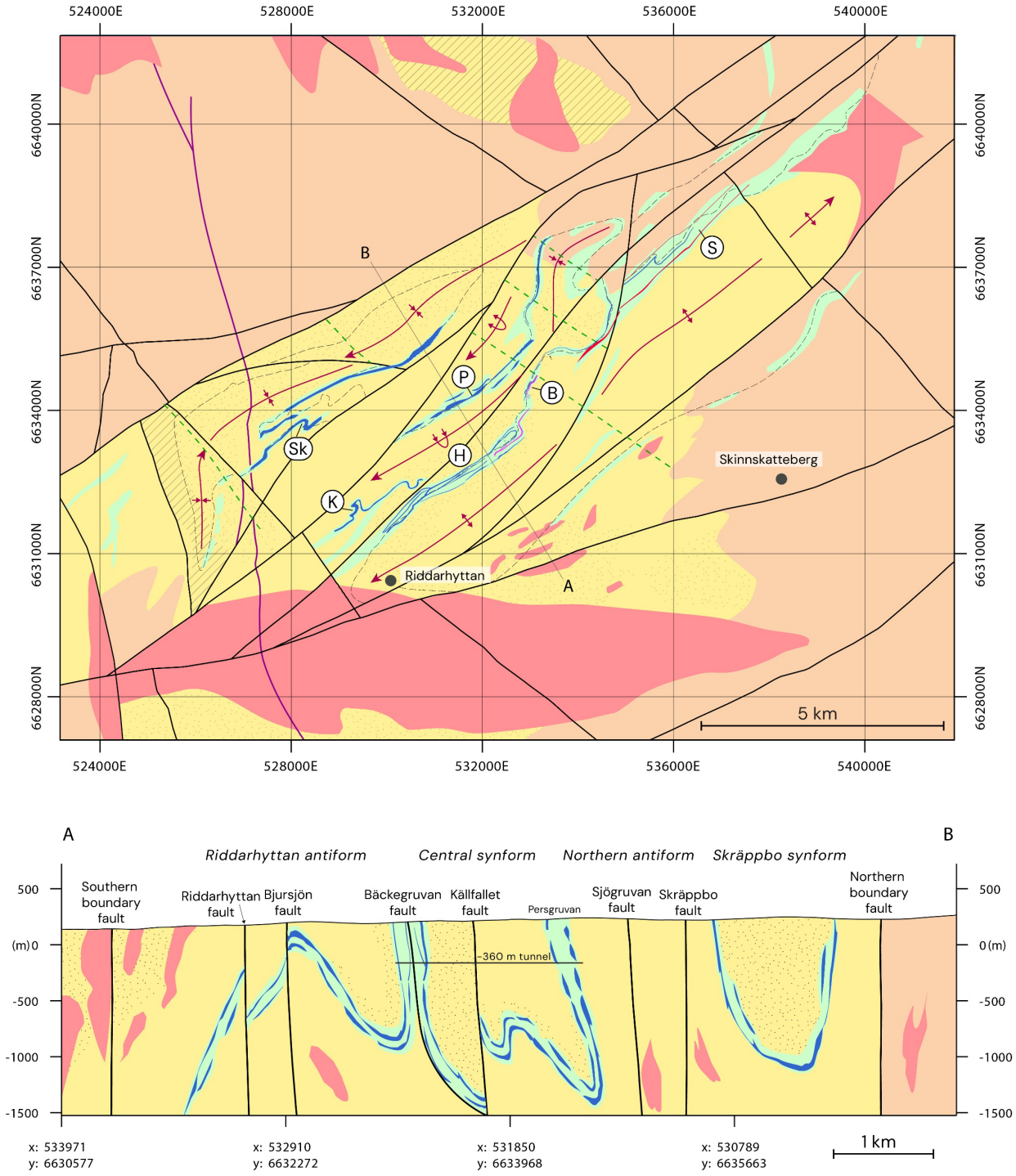

Figure 24. Geological map and corresponding cross-section interpreted from 3D modelling results from this study.

Conceptual kinematic model

Based on the structural interpretations presented earlier in this report, we propose a conceptual kinematic model to explain the structural evolution of the Riddarhyttan area. The dynamic model can be best illustrated by a theoretical experiment where a single layer is folded and refolded by three deformation phases (D2–D4) (Fig. 25). The model set-up encompasses a horizontal rope, which represents a pre-D2 fabric (S_0-S_1) containing the labels related to the major mineral deposits of the Riddarhyttan Ore Field. The rope is fixed by a spike to the right but is unconstrained to the left allowing for folding and unfolding under bulk shortening, shearing and extension. Notice that the left-to-right order of the deposit labels is an important result from running the same experiment in reverse (top view in Fig. 25), thus, starting with the present-day structural configuration. However, from a structural geological evolution perspective it makes more sense to present the model from the beginning.

During D2 E–W transpression, the first stage of deformation is dominated by dextral shearing and lateral shortening that initiate the formation of two F_{2a} drag folds. These F_{2a} folds have an overall Z-asymmetry.

With ongoing shearing, the F_{2a} drag folds grow in amplitude meanwhile they propagate forward in the direction of the confinement (spike). As a result, the mineral deposit labels become successively part of the propagating fold. Notice that some mineral deposits even migrate from one-fold limb via the fold hinge zone towards the opposing fold limb. Such "migration path" would have led to strong variations in the local stress field around the mineral deposit, causing switching between tensional and compressional, continuously deforming and re-shaping the ore bodies.

With continued shearing, the F_{2a} folds eventually become refolded by F_{2b} folds. This superimposed folding was most intense in the Central Domain and is visualised in more detail in figure 26. A noteworthy result of superimposed folding by progressive shearing is the refolding of parasitic folds by folds with contrasting asymmetries. For example, the Z-fold that has been refolded by an S-fold at Korphytte-Bastnäs as interpreted by Ihre & Sädbom (1986), can be explained by this type of progressive deformation. We even suggest that similar superimposed folding is responsible for the arrangement of multiple parallel ore lenses at Bäckegruvan. Likewise, Z-folds that have been refolded by Z-folds may explain the local thickening and pinch-out of several magnetite lenses at Persgruvan.

With further shortening, deformation becomes more localised along the major shear zones. As they grow in length, these shear zones or faults envelop fault blocks and merge into the Northern and Southern boundary faults. Stacking of the resulting fault blocks gives rise to the formation of a fault duplex.

All through D3, the maximal horizontal shortening direction becomes oriented towards N–S and results in transpression and possibly also into E–W transtension. In either case, the Riddarhyttan area undergoes sinistral shearing where pre-existing faults now accommodate sinistral slip. Some new faults form as well. In addition, F_3 folds develop as NW-trending, open upright folds. This F_3 buckling refolds the earlier F_2 folds only gently and locally, but on a larger scale F_3 folding may be responsible for some observed regional dome structures (see also Beunk & Kuipers 2012).

At D4, the region underwent N–S shortening, resulting at Riddarhyttan in the formation of several conjugate fault sets from which the NW-striking faults are newly formed. Deformation was localised along brittle faults, but some fold amplification and block rotation may have occurred as well.

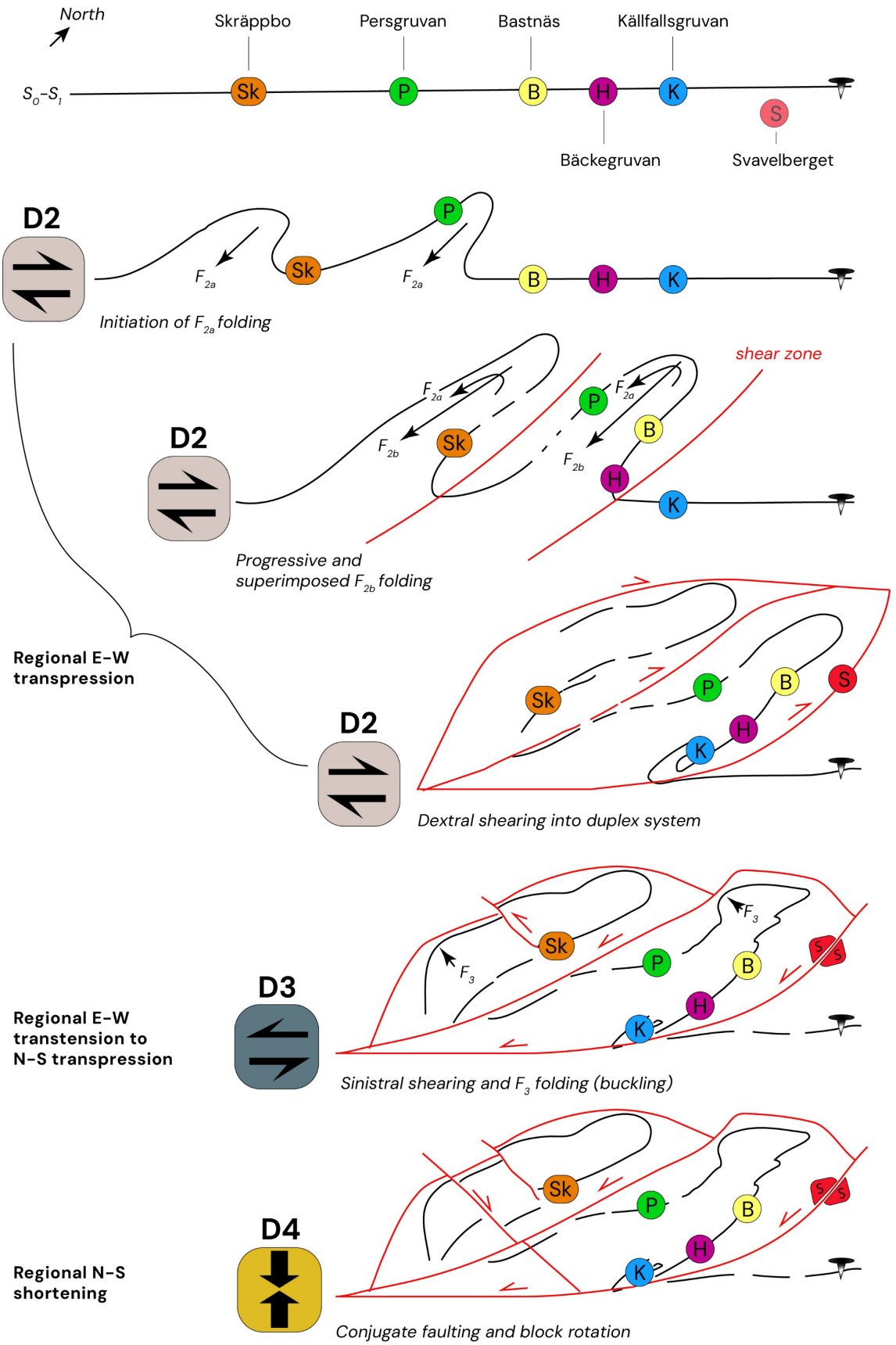

Figure 25. Conceptual kinematic model of progressive deformation at Riddarhyttan. Imagine the black line representing a rope fixed on one side. The model should be viewed as a map. See the main text for more information.

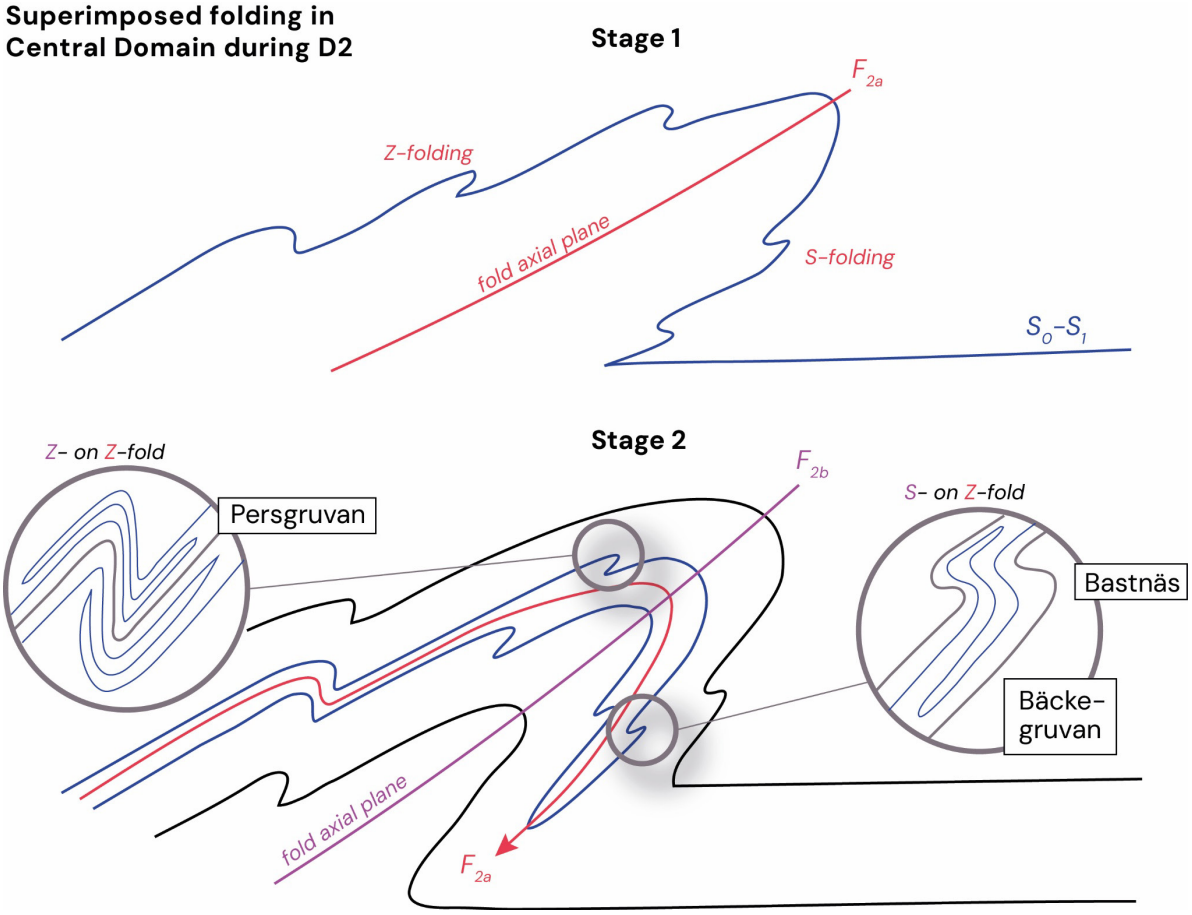

Figure 26. Zoom-in on the first stage of the conceptual kinematic model shown in Fig. 25. Superimposed folding during D2 finally results in re-folding of parasitic folds with an opposing asymmetry. The model should be viewed as a map view where the fold axis plunge is around 60–70°.

In accordance with the literature at present, our proposed deformation history commences with D1, during which tight, isoclinal folding (F_1) affected the entire Bergslagen lithotectonic unit and formed planar and linear fabrics (e.g. Stålhös 1981). At Riddarhyttan, like in many other places throughout Bergslagen, these D1 fabrics are hard to recognise due to recrystallisation and the transposition of these structures into D2–D3 fabrics. As such, D2 is generally considered in literature as the first recognisable deformation phase with progressive F_2 folding and shearing (S_2 + $L_{stretch}$) along high strain zones, such as the West Bergslagen Boundary Zone (e.g. Beunk & Kuipers 2012; Stephens & Jansson 2020; Luth et al. 2022). This phase was followed by D3, wherein the maximum shortening direction changed from E–W to N–S. Besides local refolding along upright folds, D3 transpression is considered accountable for crustal-scale buckling and orocline formation throughout the Fennoscandian shield (e.g. Lahtinen et al. 2023a, 2023b). Beunk & Kuipers et al. 2012 assigned D3 to solely E–W transtension, reserving D4 for subsequent N–S transpression and orocline formation. In our study, D4 is primarily brittle and post-dates metamorphism and ductile deformation.

Minor local and regional contradictions exist in shortening directions and timing of the different deformation phases in the literature (e.g. Stålhös 1981, Stephens & Jansson et al. 2020, Luth et al. 2022). A complete review of this is desirable but beyond the scope of this study.

Ore genetic model

Based on our modelling results and with the input from earlier studies, we sympathise with earlier genetic models postulating that mineralisations of the Riddarhyttan Ore Field formed from hot hydrothermal fluids which reacted with carbonate layers (e.g. Holtstam et al. 2014; Sahlström et al. 2019). These authors also argue that the hydrothermal fluids had a predominantly magmatic origin and infiltrated through a volcano-sedimentary succession deposited between 1.9 and 1.88 Ga within a shallow marine back-arc basin.

We further extend the above genetic model toward the whole Riddarhyttan Ore Field (Fig. 27). Local fluid pathways developed along syn-sedimentary normal faults as well as along lithological contacts, leading to skarn formation and mineralisation. The REE-rich Bastnäs deposit and the large, polymetallic Bäcke- and Östergruvan (Fe-Cu-Co-Mo) formed most likely in the nearest vicinity of a major fault zone that acted as the main pathways for hydrothermal fluids and magmatic intrusions at depth. The relatively high gravity anomaly around Bastnäs is supporting this theory (see also Fig. 6). Further away from the fault zone, metal enriched fluids migrated mainly horizontally along the volcanite-limestone boundaries. These fluids finally percolated upward into the limestone along local structures, such as fractures, boudins, or sedimentary structures related to facies changes such as volcanic interbeds, channels and pinch outs. We suggest that it was along these structures at more distal locations the mineralisation of Persgruvan, Källfallsgruvan, and Skräppbo formed. Notice that the lateral sequence of these deposits is inferred primarily from the kinematic model presented in the previous section. However, the polymetallic character of both Bastnäs and Bäckegruvan compared to the more magnetite dominated deposits of Källfallsgruvan, Persgruvan and Skräppbo can be interpreted as the result of chemical and compositional changes when moving laterally from proximal to more distal to the feeder. Finally, remobilization of metals as well as the modification of orebody geometry was caused by subsequent metamorphism and polyphase deformation (see also Figs. 25–26).

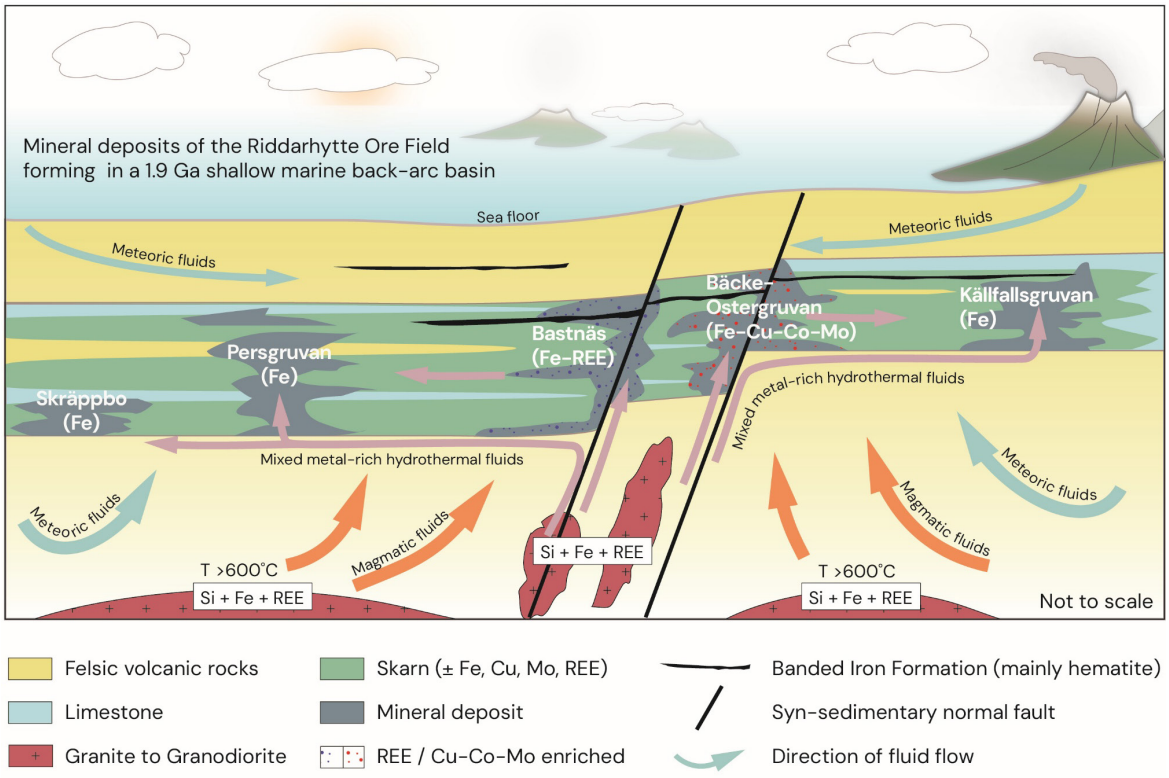

Figure 27. Proposed ore genetic model for the Riddarhyttan ore field. The cartoon is schematically drawn as a 2D cross-section projected on a 3D background. Blue and red dots within some mineral deposits refer to more intense REE- and sulfide mineralisation, respectively.

A future resource?

A resource estimate for Bäckegruvan which was updated one year before operations stopped, shows a remaining tonnage of 7.5 million tonnes at 34.4% Fe and an additional 0.67 million tonnes of low-grade iron-ore with 0.37% Cu (Bergquist 1985). At Persgruvan, a remaining tonnage of 2.8 million tonnes at 35.5% Fe was estimated. In addition, the remaining ore in other parts of the Riddarhyttan Ore Field was estimated as an inferred resource to 14.5 million tonnes. Tonnage and grade information about REE and cobalt was not included in the historic ore estimate. In 2020, however, SGU published the results from new geochemical analysis and hyperspectral scanning on 54 drill core sections form several mines in the Riddarhyttan area as well as on 17 samples from the tailings at Källfallsgruvan and Bäckegruvan (Hallberg & Reginiussen 2020). From their reconnaissance study it was concluded that the Riddarhyttan Ore Field potentially has at least 25 million tonnes of ore and 7.45 million tonnes of tailings with elevated grades of iron, manganese, copper, cobalt, molybdenum, and REE. The highest concentrations from drill core at Bäckegruvan yielded 41% Fe, 0.28% Cu, 0.29% Mo, 0.02% Co and 1.68% REE. At Källfallsgruvan up to 42% Fe was measured. Results from Persgruvan peaked at 59% Fe, 0.28% Cu, 0.02% Co and 0.82% REE. Comparable concentrations of Fe, Cu, Co and a strong variation in REE, were also obtained from rock samples taken from mine waste piles, and mineralisation found in trial pits and outcrops (Jonsson & Högdahl 2013; Sadeghi 2019; Söderhielm et al. 2023). Additional exploration drilling results presented by EMX Royalty in 2020 show the highest gold concentration drilled in the area below Pellegruvan, reaching 0.75 g/t.

Based on information from drilling, geophysics and geological investigations it was assumed by Fagersta Bruk (1978) that the orebodies continue below the current mined level and to the north. From our 3D modelling results we can support this assumption as very likely. Moreover, the revealed folding and faulting patterns suggest that the stratigraphy in which the mineralisations are bound is repeated multiple times within the Riddarhyttan area, locally exceeding depths of 1,000 meters below the surface. Its patchy character, however, makes it hard to correlate the mineralisation in areas of sparse drilling and to make a resource estimation for the area.

The scope of this study has been to present a structural framework including local models of the main mineralisations. The results show that a large quantity of economically valuable metals is very likely to be present within the Riddarhyttan Ore Field. With the present-day technology on deep mining and metal extraction considered, the mineral potential of the area is high. However, the volumes obtained from this modelling study are coarse and should therefore not be used for any kind of resource estimation without additional refinement first. Such a refined model may be based on subclassifications of the different ore-, alteration-, and rock-types. Additional geochemical modelling using assay data may also assist in enhancing the geological model and creating new drill targets. Likewise, geophysical modelling, including seismics, may reduce significantly the uncertainties of the depth extent and 3D geometry of the mineralisations and deformation zones.

Conclusions

3D geological modelling reveals the extent and geometry of the ore deposits and individual orebodies at Riddarhyttan. Their unique shapes can be considered the result of deformation exerted on multiple scales. As such, Källfallsgruvan is located in the thickened hinge zone of a vertical S-fold, the orebodies of Persgruvan occur as megaboudins, Bastnäs is in the limb of a vertical S-fold refolding a Z-fold, Bäckegruvan is situated at a fault zone cutting through a very tight, upright antiform, Skräppbo lies on the refolded limb of a large doubly plunging synform, and finally Svavelberget comprising a discordant and brecciated sulfide vein. All within a lateral distance of 10 kilometers.

From the modelling results we can postulate that most of the orebodies continue below their current mined levels. Strong indications exist in particular for Bäckegruvan and Östergruvan, but the other deposits are also open at depth. In addition, we infer from the conceptual model that the magnetite skarns locally exceed depths of 1,000 meters below the surface. We further presume that folding and faulting repeatedly expose the same mineralised horizon throughout the Riddarhyttan area.

3D modelling proved to be a useful tool to visualise and understand the polyphase tectonic evolution of the area. The resulting tectonic model encompasses superimposed folding during D2 and D3 transpressional shearing, which evolved into a strike-slip duplex. Unfolding and backstripping of the duplex in a conceptual kinematic model reveals that the major iron mineralisations around Riddarhyttan are hosted by the same stratigraphic horizon. Subsequently, we propose an ore genetic model where the Riddarhyttan Ore Field formed from hot hydrothermal fluids that reacted with carbonate layers. This model is consistent with former concepts from earlier studies, however, we emphasise the importance of various fluids and their pathways related to major structures (e.g. faults), stratigraphic contacts (limestone-volcanic rock), and minor structures within the carbonate layers (e.g. fractures, boudin necks). Bäckegruvan and Bastnäs were likely connected to major faults allowing these deposits to become also enriched in Co-Cu and REE, respectively. Similarly, the differences in mineralogy and chemical composition between the Fe-oxide deposits at Riddarhyttan presumably originate from a certain fluid composition related to their primary source, but also to their pathways.

The purpose of this study was to obtain a multi-scale structural framework for the Riddarhyttan area. The results show that a large quantity of valuable metals is very likely to be present today within the Riddarhyttan Ore Field. However, the area's complex architecture required model simplification mainly to balance between clarity and level of detail. It is therefore recommended to use the presented models for targeting and resource estimation only after additional input and constraints from drilling, site investigations, geophysical and geological modelling.

Acknowledgements

The authors want to thank Hein Raat, formerly at EMX Royalty, and his colleagues for sharing his ideas, geological- and geophysical datasets and introduction to the field area. Bengt Högrelius for digitising the drill logs from the Bastnäs tunnel. Edna Spahic for sharing her structural measurements and her orebody model of Källfallsgruvan. Tobias Kampmann from (LTU) and Alexander Lewerentz (SGU) for their efforts in the field and lively discussions at the local pizzeria.

References

Allen, R.L., Lundstrom, I., Ripa, M., & Christofferson, H., 1996: Facies analysis of a 1.9 Ga, continental margin, back-arc, felsic caldera province with diverse Zn-Pb-Ag-(Cu-Au) sulfide and Fe oxide deposits, Bergslagen region, Sweden: *Economic Geology, v. 91, no. 6*, pp. 979–1008.

Ambros, M., 1983a: Berggrundskartan 11F Lindesberg NO. *Sveriges geologiska undersökning Af 141*.

Ambros, M., 1983b: Beskrivning till berggrundskartan 11F Lindesberg NO. *Sveriges geologiska undersökning Af 141*, p. 75.

Andersson, S.S., Jonsson, E. & Sadeghi, M., 2024: A synthesis of the REE-Fe-polymetallic mineral system of the REE-line, Bergslagen, Sweden: New mineralogical and textural-paragenetic constraints. *Ore Geology Reviews, 174*, p.106275.

Bergquist, E., 1982–1985: Karta över Bäckegruvan belägen inom Skinnskattebergs kommun, Västmanlands län. Tillgängligt via Sveriges geologiska undersökning. Gruvkarta och beskrivning No SK4UA-B. Bergmästaren i södra distriktet, Falun, J1f:16–17.

Bergquist, E., 1985: Beskrivning till slutkartor över delar av Riddarhytte malmfält i Skinnskattebergs kommun och socken, Västmanlands län. Tillgängligt via Sveriges geologiska undersökning. Bergmästaren i södra distriktet, Falun, F6:16

Beunk, F.F. and Kuipers, G., 2012: The Bergslagen ore province, Sweden: Review and update of an accreted orocline, 1.9–1.8 Ga. *Precambrian Research, v. 216*, pp. 95–119.

Dunst, R., Pitcairn, I., Raat, H., Jansson, N.F., Karlsson, A., 2024: A lithological context for stratabound REE mineralisation at the birthplace of REE – Bastnäs, Riddarhyttan, Sweden. *Abstract volume Nordic Geological Winter Meeting* in Göteborg, pp. 143.

European Commission, 2023: *Critical Raw Materials: ensuring secure and sustainable supply chains for EU's green and digital future.* <https://ec.europa.eu/commission/presscorner/detail/en/ip_23_1661> Last accessed March 6, 2026.

Fredriksson, E., 1932–1984: Karta över Hans Urbansons fält beläget inom Riddarhytte Malmfälts odalutmål i Skinnskattebergs socken, Västmanlands län. Tillgängligt via Sveriges geologiska undersökning. Bergmästaren i södra distriktet Falun, J1f:19.

Geijer, P., 1921: The cerium minerals of Bastnäs Riddarhyttan. *Sveriges geologiska undersökning C304*, pp. 24.

Geijer, P. & Carlborg, H., 1923: Riddarhytte malmfält i Skinnskattebergs socken, Västmanlands län. Kungl. Kommerskollegium, 343 s.

Geijer, P. & Magnusson, N.H., 1944: De mellansvenska järnmalmernas geologi. *Sveriges geologiska undersökning Ca 35*, 654 s.

Haag, J., Pitcairn, I., Lewerentz, A., Jansson, N-F., Eigler, M. & Raat, H., 2022: Mineralization and alteration paragenesis of Fe-oxide-sulfide-REE mineralization in the Bastnäs area, Bergslagen ore district, Sweden. *Abstract volume Nordic Geological Winter Meeting* in Reykjavik, pp. 126.

Hallberg, A. & Reginiussen, H., 2020: Critical Raw Materials in ores, waste rock and tailings in Bergslagen. *SGU-rapport 2020:38*, Sveriges geologiska undersökning, p. 60.

Hedberg, N., 1897–1923: Karta öfver Lerklocka jernmalmsgrufva jämte närgränsande fyndigheter belägna i Vestra delen af Morbergsfältet inom Riddarhytte malmfälts odalutmål, Skinnskattebergs socken af Vestmanlands Län. Gruvkarta No 424. Tillgänglig via Sveriges geologiska undersökning. Bergmästaren i östra distriktet, JIIId:92.

Holtstam, D., Grins, J. & Nysten, P., 2004: Håleniusite-(La) from the Bastnäs deposit, Västmanland, Sweden: a new REE oxyfluoride mineral species. *Canadian Mineralogist 42*, pp. 1097–1103.

Holtstam, D., Andersson, U.B., Broman, C. a& Mansfeld, J., 2014: Origin of REE mineralization in the Bastnäs-type Fe-REE-(Cu-Mo-Bi-Au) deposits, Bergslagen, Sweden. *Mineralium Deposita*, *49*, pp. 933–966.

Ihre, P. & Sädbom, S., 1986: Riddarhytte malmfält prospekteringsarbeten 1986, del 1–3. *Sveriges geologiska AB* Prospekteringsrapport PRAP86541, p. 478.

Kamb, W.B., 1959: Ice petrofabric observations from Blue Glacier, Washington in relation to theory and experiment: *Journal of Geophysical Research, v. 64, no. 11*, pp. 1891–1909.

Jonsson, E. & Högdahl, K., 2013: New evidence for the timing of formation of Bastnäs-type REE mineralisation in Bergslagen, Sweden. *Mineral Deposit Research for a High-Tech World – Proceedings of the 12th Biennial SGA Meeting*, 1724–1727.

Lahtinen, R., Köykkä, J., Salminen, J., Sayab, M. & Johnston, S.T., 2023a: Paleoproterozoic tectonics of Fennoscandia and the birth of Baltica. *Earth-Science Reviews*, *246*, 104586.

Lahtinen, R., Köykkä, J. & Kurhila, M., 2023b: Tectonic evolution of a Paleoproterozoic diffuse cryptic suture zone in northern Fennoscandia and the correlation of northern Fennoscandia and southern Greenland. *Journal of the Geological Society*, *180*(5), 2023-007.

Linders, W., 2016: *U-Pb geochronology and geochemistry of host rocks to the Bastnäs-type REE mineralization in the Riddarhyttan area, west central Bergslagen, Sweden*. Master thesis, Lund University.

Luth, S., Sahlström, F., Bergqvist, M., Hansson, A., Lynch, E.P., Sädbom, S., Jonsson, E., Andersson, S.S. & Arvanitidis, N., 2022: Combined X-ray computed tomography and X-ray fluorescence drill core scanning for 3-D rock and ore characterization: Implications for the Lovisa stratiform Zn-Pb deposit and its structural setting, Bergslagen, Sweden. *Economic Geology*, *117*(6), pp.1255–1273.

Malmgren, E., 1910–1984: Karta öfver Öfra och Nedra Persgrufvorna i Skinnskattebergs socken och Västmanlands län. Upprättad efter mätning afslutad den 25 november 1910. Gruvkarta 615. Tillgängligt via Sveriges geologiska undersökning. Bergmästaren i södra distriktet Falun Jif:18.

Mannerstråle, C.H., 1886–1910: Karta öfver Bastnäs Gruvefält i Skinnskattebergs Bergslag af Westerås län. Upprättad efter mätning afslutad den 4 Augusti 1886. Gruvkarta 111. Tillgängligt via Sveriges geologiska undersökning. Bergmästaren i östra distriktet JIIId:84.

Mörtsell, K., 1921–1957: Karta över Myrbacksfältet i Skinnskattebergs socken Västmanlands län. Tillgängligt via Sveriges geologiska undersökning. Gruvkarta No 725C. Bergmästaren i östra distriktet JIIId:93.

Mörtsell, K., 1927–1953: Karta över Östergruvan inom Riddarhytte malmfälts odalutmål i Skinnskattebergs socken Västmanlands län. Gruvkarta No 758-C. Tillgängligt via Sveriges geologiska undersökning. Bergmästaren i södra distriktet Falun J1f:13.

Raat, H., 2020: Riddarhyttan Technical Report Greenfield Exploration 2019. *Internal report EMX Royalty corp.*

Sadeghi, M. (ed.), 2019: Rare earth elements distribution, mineralisation and exploration potential in Sweden. *Rapporter och meddelanden 146*, Sveriges geologiska undersökning, p. 184.

Sahlström, F., Jonsson, E., Högdahl, K., Troll, V.R., Harris, C., Jolis, E.M. & Weis, F., 2019: Interaction between high-temperature magmatic fluids and limestone explains 'Bastnäs-type' REE deposits in central Sweden. *Scientific Reports*, *9(1)*

Spahic, E, 2021: *Three-dimensional modelling of the Källfallsgruvan iron oxide deposit, Riddarhyttan ore field, Bergslagen, Sweden: Integrating existing and new data to aid understanding of structural controls on mineral exploration.* Masters degree thesis, Luleå Tekniska Universitet, Sweden. pp. 47.

Söderhielm, J., Larsson, D., Bergman, T., Hellström, F., Nysten, C., Jonsson, E., Hildebrand, L. & Berggren R., 2023: Malmer, industriella mineral och bergarter i Skinnskattebergs kommun, Västmanlands län. *Rapporter och meddelanden 153*, Sveriges geologiska undersökning, p. 263.

Stephens, M.B., & Jansson, N.F., 2020: Paleoproterozoic (1.9–1.8 Ga) synorogenic magmatism, sedimentation and mineralization in the Bergslagen lithotectonic unit, Svecokarelian orogen: *Geological Society, London, Memoirs, v. 50*, pp. 155–206, doi: 10.1144/M50-2018-17.

Stålhös, G., 1981, A tectonic model for the Svecokarelian folding in east central Sweden: *Geologiska Föreningen i Stockholm Förhandlingar, v. 103, no. 1*, pp. 33–46.

Sundholm, H., 1899–1971: Karta öfver Källfallsgrufvan inom Södra Skilåfältet i Skinnskattebergs socken Vestmanlands län. Tillgängligt via Sveriges geologiska undersökning. Bergmästaren i östra distriktet JIIId:94.

Tegengren, F.R., 1912: Järnmalmstillgångarna i mellersta och södra Sverige. Utredning verkställd åren 1907–1909. *Sveriges geologiska undersökning Ca 8*, pp. 257.

Tegengren, F.R., 1924: Sveriges ädlare malmer och bergverk. *Sveriges geologiska undersökning Ca 17*, pp. 406.